ANCR-1120

NASA CR-121190

FEASIBILITY STUDY OF FULL-REACTOR GAS CORE DEMONSTRATION TEST

J. F. Kunze
J. H. Lofthouse
C. J. Shaffer
P. J. Macbeth

Prepared for
NATIONAL AERONAUTICS AND SPACE ADMINISTRATION
Contract C-59718B

R. E. Hyland, NASA-LEWIS
Technical Project Manager

Date Published - June 1973

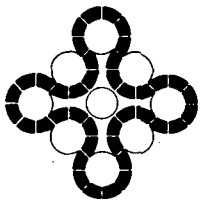

Aerojet Nuclear Company
NATIONAL REACTOR TESTING STATION
Idaho Falls, Idaho - 83401

Printed in the United States of America
Available from
National Technical Information Service
U. S. Department of Commerce
5285 Port Royal Road
Springfield, Virginia 22151
Price: Printed Copy $5.45; Microfiche $0.95

1. Report No.	2. Government Accession No.	3. Recipient's Catalog No.
NASA CR-121190		

4. Title and Subtitle	5. Report Date
Feasibility Study of Full-Reactor Gas Core Demonstration	June 1973
	6. Performing Organization Code
7. Author(s)	8. Performing Organization Report No.
J. F. Kunze, J. H. Lofthouse, C. J. Shaffer, P. J. Macbeth	ANCR-1120
	10. Work Unit No.
9. Performing Organization Name and Address	11. Contract or Grant No.
Aerojet Nuclear Company Idaho Falls, Idaho 83401	C-59718B
	13. Type of Report and Period Covered
12. Sponsoring Agency Name and Address	Contractor Report
National Aeronautics and Space Administration Washington, D.C. 20546	14. Sponsoring Agency Code

15. Supplementary Notes

Technical Project Manager, R. E. Hyland, Advanced Concepts Branch, NASA Lewis Research Center, Cleveland, Ohio 44135

16. Abstract

Separate studies of nuclear criticality, flow patterns, and thermodynamics for the gas core reactor concept have all given positive indications of its feasibility. However, before serious design for a full scale gas core application can be made, feasibility must be shown for operation with full interaction of the nuclear, thermal, and hydraulic effects. This report considers a minimum sized, and hence minimum expense, test arrangement for a full gas core configuration. It is shown that the hydrogen coolant scattering effects dominate the nuclear considerations at temperature. A cavity diameter of somewhat larger than 4 ft (122 cm) will be needed if temperatures high enough to vaporize uranium are to be achieved.

17. Key Words (Suggested by Author(s))	18. Distribution Statement
Gas Core Reactor High Temperature Test Hot Hydrogen Effect	Unclassified - Unlimited

19. Security Classif. (of this report)	20. Security Classif. (of this page)	21. No. of Pages	22. Price*
Unclassified	Unclassified		$5.45

* For sale by the National Technical Information Service, Springfield, Virginia 22151

ACKNOWLEDGEMENTS

The authors wish to express appreciation for the careful review and advice received from Dr. R. M. Brugger, and for the analytical help and support received from B. L. Rushton. Dr. H. L. McMurry was responsible for the molecular binding functions from which the hydrogen scattering cross sections were developed.

TABLE OF CONTENTS

		Page
1.0	SUMMARY	1
2.0	INTRODUCTION	2
3.0	NUCLEAR DESIGN	7
	3.1 Cross Section Detail	9
	3.2 Criticality Calculations	15
	3.3 Temperature Coefficient	35
	3.4 Summary of Nuclear Results	41
4.0	THE CLOSED CYCLE TEST SYSTEM	43
	4.1 Materials Selection	43
	4.2 Choice of Coolant Gas	44
	4.3 The Gas Cycle	47
	4.4 The Gas-Uranium Separation System	50
	4.5 Cavity Wall Thermal Hydraulics	51
5.0	OPERATING CHARACTERISTICS	53
	5.1 Power Levels and Temperatures	53
	5.2 Radiation Levels	54
	5.3 Test Changes, Servicing and Maintenance	54
	5.4 Diagnostics	55
6.0	COST AND SCHEDULE ESTIMATES	56
7.0	CONCLUSIONS AND RECOMMENDATIONS	59
REFERENCES		61

FIGURES

2.1	Schematic drawing of Gas-core nuclear rocket concept	3
3.1	Gas Core Test Reactor	8
3.2	Neutron angular distribution at several H_2 temperatures	11

TABLE OF CONTENTS

(Continued)

Page

FIGURES (Cont'd)

3.3 Total neutron scattering cross section for several H_2 temperatures 12

3.4 NASA 70 cm cavity reactor fuel density distribution 500 atm pressure case 27

3.5 NASA 70 cm cavity reactor hydrogen coolant-propellant density distribution 28

3.6 NASA temperature distribution for 70 cm cavity reactor 500 atm case 29

3.7 MONA - NASA specification results K_{eff} vs volume fraction at constant radius ratio 30

3.8 MONA - NASA specification results K_{eff} vs cavity radius at constant radius ratio. 31

3.9 MONA - NASA specification results K_{eff} vs fuel pressure at constant configuration and constant hydrogen parameters. . . 32

3.10 MONA - NASA specification results K_{eff} vs R_{eff} at changing fuel mass. 33

3.11 MONA - NASA specification results K_{eff} vs R_{eff} at constant radius ratio 34

3.12 Plot of some thermal neutron group flux data vs reactor radius through core and hydrogen containing regions for Case 4 38

4.1 Closed Cycle Test System 48

TABLES

3.1 Neutron Energy Group Structure Used in Transport Calculations 10

3.2 Dimensionless Concentration of Hydrogen at Pressures and Temperatures of Interest 14

3.3 Model for Calculation of Base Reactor - Case No. 1 16

TABLE OF CONTENTS

(Continued)

Page

TABLES (Cont'd)

3.4 Calculational Case Descriptions and Calculated Eigenvalues 17

3.5 S_4 Transport Code-19 Energy Groups, Full Upscattering in 7 Thermal Groups 24

3.6 200 Atmospheres - NASA Specifications - Base Case No. 2 . 25

3.7 Summary of NASA Specification Calculations 26

3.8 P_o Group to Group Scattering Matrix for Hot and Cold H_2. . 37

3.9 Nominal Total Scattering Cross Sections and Scattering Mean Free Path for Thermal Neutrons in H_2. 39

4.1 Materials Selection. 45

4.2 Characteristics of Coolant Gases 46

6.1 Primary Construction Costs of 4 ft Cavity Demonstration Reactor. 57

6.2 Operating Costs. 58

1.0 SUMMARY

This report considers the feasibility of a small scale, but still full-operating gas core reactor demonstration test. The report compares the operating conditions, test results and costs with those of the "Mini-Cavity" demonstration concept.

The small scale, full-reactor concept using hydrogen coolant involves a strong dependence of maximum available discharge temperature on cavity size. A 4-ft diameter cavity, for instance, appears limited to a discharge temperature of about 4000°R. The cause of this limitation is the strong negative reactivity effect of upscattering from the hydrogen. Larger cavities will permit higher operating temperatures.

Costs of the small scale full-operating gas core reactor demonstration compare favorably with those of the "Mini-Cavity" concept, being only a nominal 25% higher than for the "Mini-Cavity." The effective demonstration of the feasibility of the gas core concept will eventually require a full-gas-core reactor test. It would therefore appear to be appropriate to perform such an experiment in a low cost small scale device and thereby bypass the Mini-Cavity demonstration, unless the latter could be conducted inexpensively in an existing reactor facility.

2.0 INTRODUCTION

The gas core nuclear rocket has long been considered the ultimate in specific impulse capability for space propulsion.[1,2] Figure 2.1 is a schematic of the concept. Recent considerations of the capabilities for this system[3] consider engines with specific impulses as high as 4400 seconds, with 6000 MW power and 10 lb/sec hydrogen propellant flow rates. Mass flow rate loss ratios of the nuclear fuel (^{235}U or ^{233}U) to that of the propellant are hoped to be in the range of 1% or less. Discharge temperatures through the nozzle of as high as 30,000°R are considered feasible[3] even though present-day chemical rocket discharges are only as high as 7500°R.

The gas core nuclear rocket concept will need to be tested at temperature in a test program on an earth-based "prototype" demonstration. Three possibilities exist for the demonstration test:

1. A loop-type (Mini-Cavity) test within a conventional test reactor driver core to test some but not all of the parameters of the full scale reactor.
2. A small scale full reactor test. A small cavity, nominally 4 ft in diameter, is envisioned which will allow a gaseous uranium core but at a reduced temperature from the full scale reactor. This test should allow testing of most parameters, and extrapolation of the remainder to the full scale reactor.
3. A full scale, 10 to 12 ft diameter cavity test, with all the characteristics of the rocket engine. This device would operate at a much higher total power than either of the other two devices.

This report discusses the second concept, with comparison being made to the first concept. The full scale 10 to 12 foot cavity diameter test

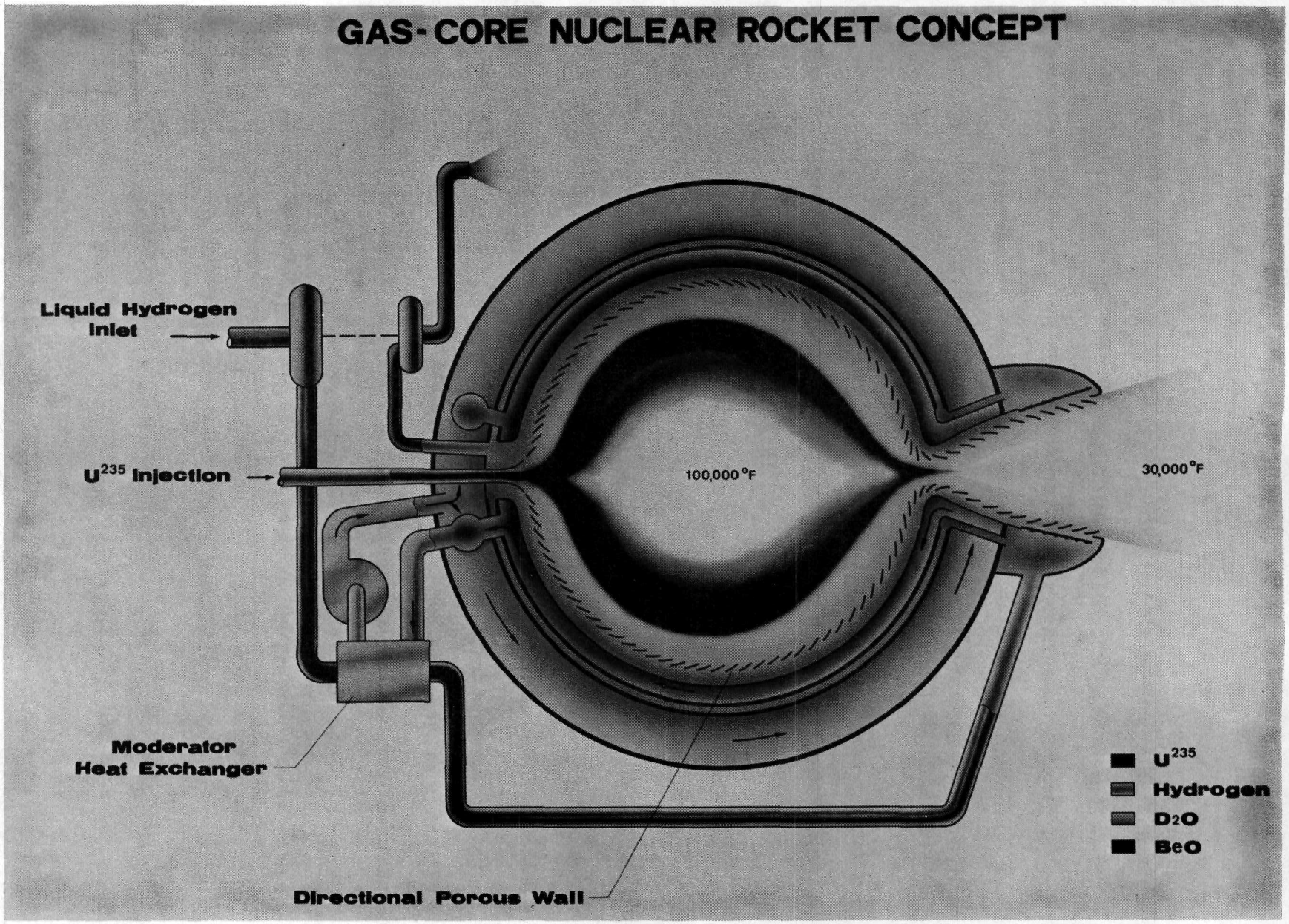

Figure 2.1 Schematic drawing of Gas-core nuclear rocket concept.

(concept No. 3) is not herein explicitly considered as a feasible alternative for the next step in gas core development. Its power level is beyond the range of a program which has yet to demonstrate completely that the gas core reactor concept is workable at low power.

With the new high performance and high coolant temperature characteristics projected for the gas core nuclear rocket, protection of the cavity walls and nozzle walls becomes a major consideration. The deliberate seeding of the hydrogen has been found to produce a radiation attenuation coefficient sufficiently large to leave tolerable radiant heat fluxes at the cavity wall. This seems to be feasible even when the radiating uranium is at 100,000°R in a 10 ft cavity. With just a small weight fraction of seed[4] (less than 1%), resulting heat fluxes at the walls can be reduced to about 100 watts/cm^2 (10^6 Btu/hr ft^2). Assuming little turbulent convective mixing, the gas core temperature can be adjusted throughout a rnage of high temperatures merely by adjusting the amount of seed and/or the flow rate of the propellant gas. Though such considerations may appear highly idealized, in principle this operating mode leads to a new concept for testing of the gas core concept in a more controllable nuclear environment.

In this new concept, the Mini-Cavity, a driver core would provide adequate thermal flux environment for the operation of a smaller than full scale test loop. This driver concept now appears feasible because the high fluxes hitherto felt to be necessary, based upon radiation of the hot gas core (100,000°R) to a relatively cold (10,000°R) non-seeded hydrogen propellant environment which required driver core thermal fluxes greater than 10^{16} n/cm^2 sec, are not necessary. To reach this flux level would require a total reactor power level for the driver in the neighborhood of 1000 MW. The new concept of supplying a highly effective temperature startified insulating blanket through seending around the gas core allows

for operation of a small (approximately 2 ft diameter) driver core loop system with fluxes in the range of 1 to 5 x 10^{14}, well within the capabilities of present test reactors. This new seeding approach makes feasible the concept of a Mini-Cavity test for an earth demonstration of the gas core concept. Temperature capabilities with the seeding are more than adequate to achieve fuel vaporization. This general concept is discussed in Reference [5], though that reference is concerned principally with the space propulsion applications of a Mini-Cavity.

The Mini-Cavity approach for a demonstration test appears to be an economically feasible method of demonstrating the operation of the gas core concept. Though component work (experiments and calculational studies) on flow, criticality, and heat transfer aspects have to date shown no lack of feasibility of the gas core concept, still these component tests have essentially been independent. They have not been put together, except for flow and thermodynamics in the rf heating work,[6] and this can be argued is significantly different in some respects from the nuclear heating driving force which the real reactor will experience. Certainly the nuclear coupling has been demonstrated to be quite strong, both because of the hydrogen scattering and because of the gas-core-to-cavity-radius ratio effects[7]. The former effect is even stronger than hitherto assumed, as is shown in this report. The Mini-Cavity concept would allow for the gas loop to contribute a significant (measureable) amount of multiplication factor of the total reactor system, say of the order of 5%Δk, while producing the order of 10% of the total system power. Still the driver reactor would have adequate control to operate by itself and to compensate for instabilities and possible reactivity excursions generated within the loop.

Despite the apparent advantages of the Mini-Cavity test concept, there are uncertainties about its outcome that still dictate the need to consider

a full gas core reactor demonstration test. Foremost among the questions pertaining to the adequacy of the Mini-Cavity concept are the following:

1. What is the extent of convective turbulent mixing in the propellant gas buffer layer and how will this alter the heat transfer characteristics from the hot gas core? A significant increase in the heat transfer coefficient would require a higher driver core flux to attain the needed power densities in the core region. Also, the maintenance of a thicker protective boundary layer would be needed to prevent burnout of the walls.

2. A loop test with its nuclear driving force provided by an outside system may fall short, in a programmatic sense, of demonstrating the complete feasibility of the gas core concept.

For these reasons, a small scale, full-reactor test at minimum size but with adequate temperatures for demonstrating the gaseous core concept is considered in this report. The goal is to balance the desired demonstration program requirements with the cost of the test. For instance, it is concluded that if a cavity size of about 4 ft diameter can be achieved, then the gas flow requirements and the loop clean-up system requirements will not be significantly greater in complexity or cost than those for the loop of the Mini-Cavity. However, for the full-reactor test to achieve its demonstration goal, the discharge temperatures must be at least in the range of NERVA discharge temperatures (4,000°R and higher) and the gas core temperatures must be great enough to vaporize uranium metal. A 11,000°R edge "core" temperature is assumed to be the minimum requirement.

3.0 NUCLEAR DESIGN

The gas core reactor nuclear design (Figure 3.1) presents some unusual reactor physics problems, of the type not encountered in conventional reactor design. Some of these are discussed in Refs. [7], [8] and [9] which deal with the correlation of room temperature critical experiments using multi-energy-group numerical calculational techniques. The principal difficulties found with the calculation of cold (near room temperature) gas core reactors were as follows:

1. The uranium core had a high ratio of absorption to scattering, making diffusion theory not applicable without the use of specially modified diffusion coefficients. Use of transport theory or transport corrected diffusion theory is essential if eigenvalue accuracies within 5% ΔK are to be achieved.
2. The scattering effects of the hydrogen propellant material (simulated) were much more important than the hydrogen absorption effects. The correct scattering kernel for the particular molecule must be used in order to obtain the correct "diffusion barrier" effect.
3. Because of the sensitivity of the results to the hydrogen scattering law, a multi-thermal group structure is required. This becomes even more important for high temperature operation where the hydrogen propellant has much higher energy than the thermal neutrons emanating from the reflector-moderator of D_2O. Multi-thermal groups, with upscattering*, create difficulties in achieving convergence of the

*In the multi-energy-group numerical calculations, solutions were made from the top energy group working down. When upscattering is present, the lower energy group fluxes from the previous iteration are the best that is available for calculation of the upscattering source terms. This results in a slow convergence on energy group fluxes as well as on spatial and angular fluxes.

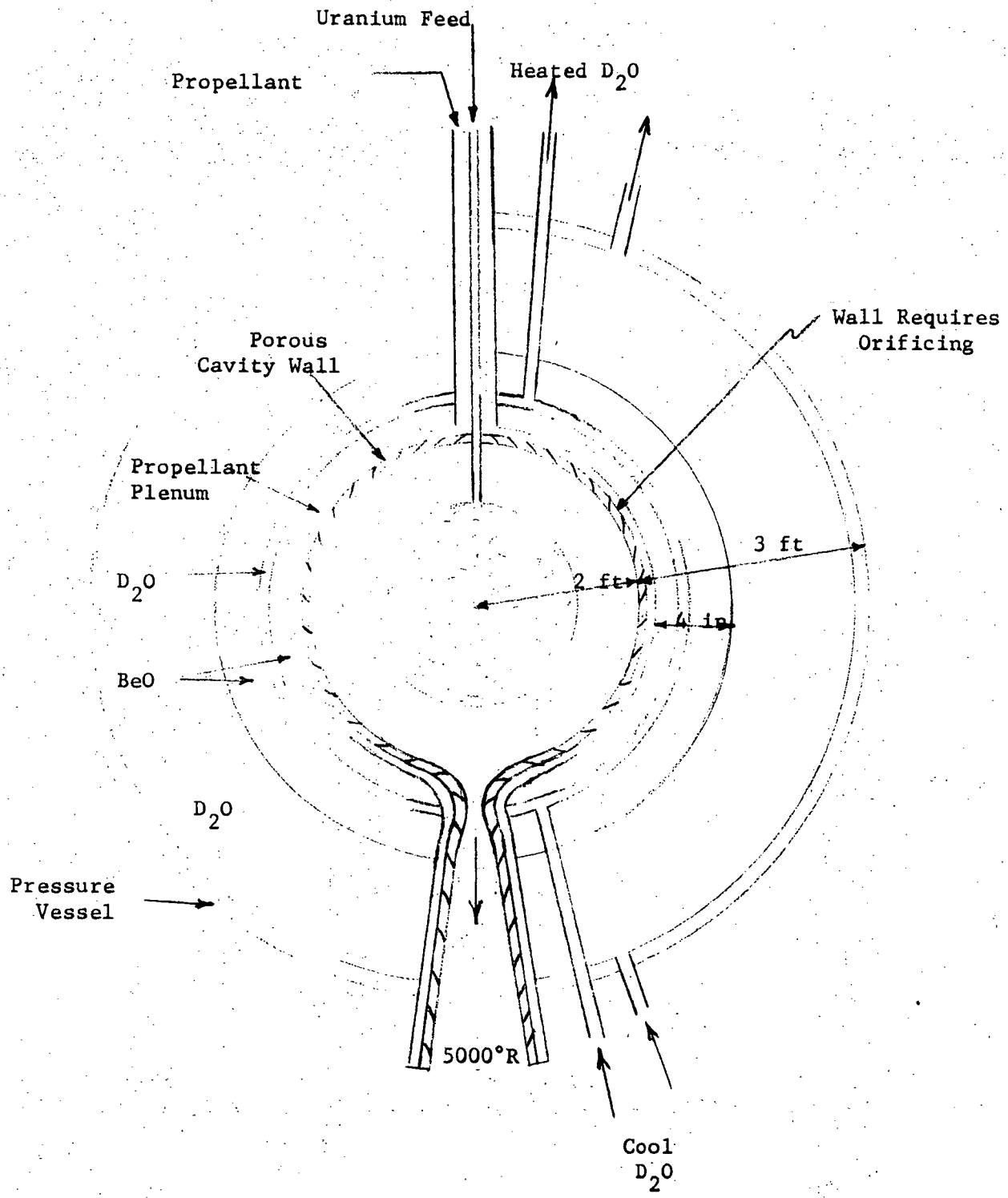

Fig. 3.1 Gas Core Test Reactor

numerical solutions. This problem is enhanced by the long mean free paths in the system and the high importance of neutrons deep in the reflector.

4. The low density core with poor scattering creates ray problem effects in two-dimensional S_n calculations where the S_n detail is small (such as 4). This, plus the long running times for two-dimensional transport problems, make such calculations too costly. One-dimensional approximations are needed to the true geometry, if computer costs are to be kept reasonable. (Ray effects do not occur in one-dimensional spherical calculations.)

The above problems can only be expected to be compounded by the transition to high temperature calculations discussed in the following sections.

3.1 Cross Section Detail

Table 3.1 lists the 19-neutron energy group structure used in the scoping study transport calculations. This structure had been adopted for the initial calculations of the cold critical experiments[8] and its use for this study was for convenience. If calculations at very high temperatures (>10,000°K) are to be made, a modified structure with finer energy groups in the 0.3 eV range will be necessary. Hydrogen group constants used in the calculations were generated for 293°K, 1000°K, 2500°K, 5,000°K, and 23,000°K.

The set of curves shown in Figures 3.2 and 3.3 illustrate the energy and temperature dependence of the total molecular hydrogen cross section and the angular scattering distribution for the several temperatures used in the calculational model. Of special significance is the drastic up-scattering effect on thermal energy neutrons by hydrogen at elevated

Table 3.1

Neutron Energy Group Structure Used in Transport Calculations

Group	Lower U	ΔU	Lower E
1 (Starts at 10	1.0	1.0	3.7 MeV
2 MeV)	1.5	0.5	2.2
3	2.0	0.5	1.4
4	3.0	1.0	0.5
5	4.0	1.0	0.18
6	5.0	1.0	67.0 KeV
7	6.0	1.0	25.0
8	8.0	2.0	3.4
9	10.0	2.0	425.0 eV
10	12.0	2.0	61.0
11	14.0	2.0	8.312
12	15.25	1.25	2.38
13	17.00	1.75	0.414
14	17.73	0.7275	0.2
15	18.24	0.5108	0.12
16	18.64	0.4055	0.08
17	19.81	1.163	0.025
18	21.42	1.609	0.005
19	(23.42)	(2.0)	0

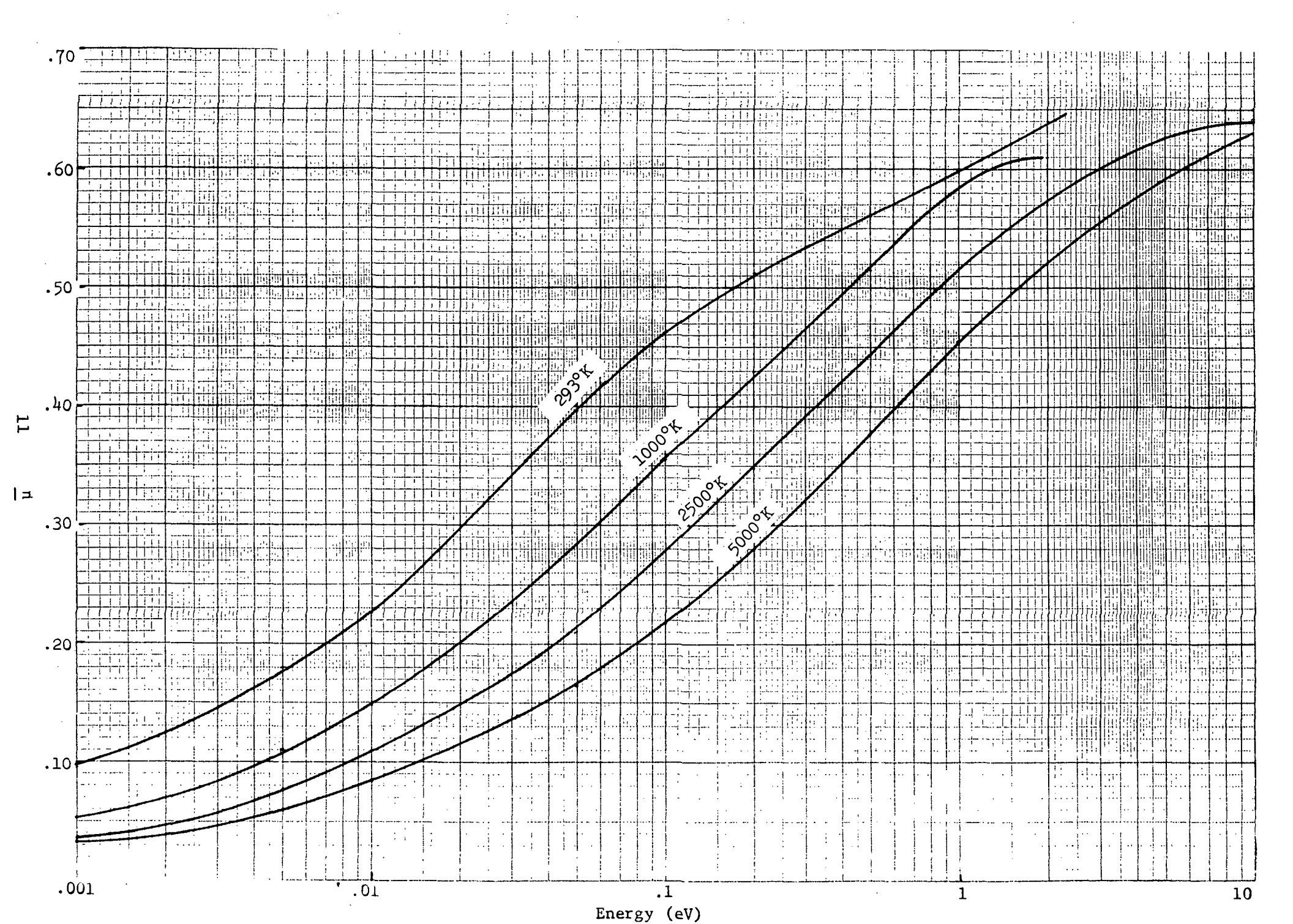

Figure 3.2 Neutron angular distribution at several H_2O temperatures.

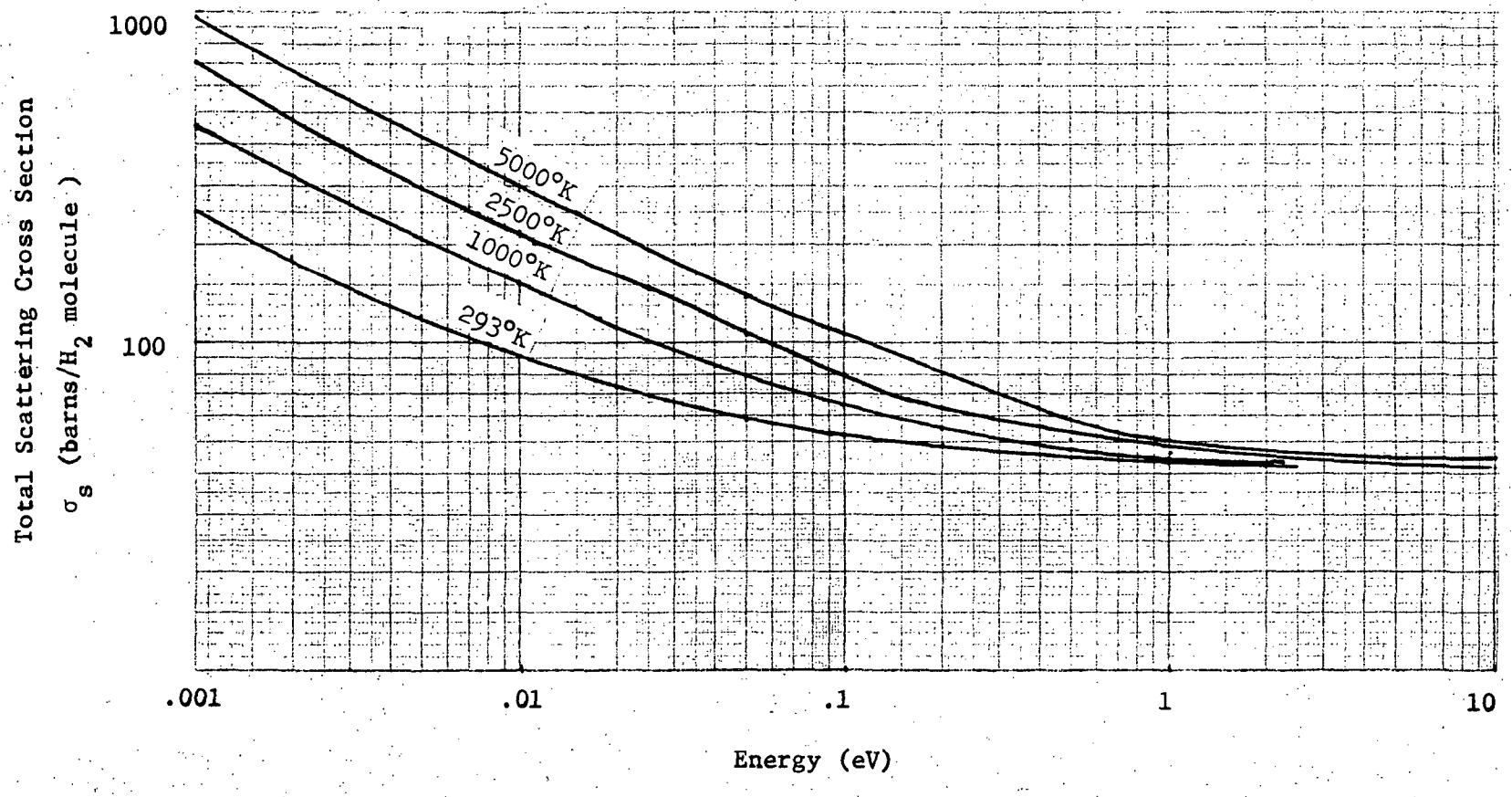

Figure 3.3 Total neutron scattering cross section for several H_2 temperatures.

temperatures. This effect has a most pronounced influence on the calculational results which will be discussed further in Section 3.3.

Although only cross section data for hydrogen molecules were used in the calculations, Table 3.2 is included to show the relative abundance of molecular hydrogen, free hydrogen atoms, and ionized hydrogen atoms at pressures of 100 and 300 atmospheres and for the temperatures used in the calculational models. These data were extracted from Ref. [10]. At 100 atmospheres pressure and 2500°K, 0.12% of the hydrogen mass is dissociated to atomic hydrogen and at 300 atmospheres the disassociated hydrogen has dropped to 0.07%. These values increase to 30.5% and 18.2%, respectively at 5000°K. As noted in the table, ionization of the hydrogen at these temperatures and pressures is minimal.

The molecular hydrogen model used for creating thermal neutron scattering kernels allows for harmonic vibration with a quantum level spacing of 0.545 eV (spring type arrangement) and the translational and rotational modes are treated classically for these dumbbell molecules. This model should be realistic and appears to give about the same total cross section vs. energy as a free atom model. Thus, at 5000°K, the amount of molecular dissociation will have a negligible effect upon the scattering properties. Kernels for each H_2 temperature mentioned above were incorporated into the library of the code INCITE[11] which calculates the thermal cross sections.

The cross section data was averaged into the group structure shown in Table 3.1 by use of the codes INCITE and PHROG[12]. These two codes are *modifications of the commonly available industrial user codes GATHER*[13] and GAM[14] used for obtaining thermal and fast-intermediate cross sections, respectively. The transition of the scatter transfer matrices between the two codes is done for the Po matrices

Table 3.2

Dimensionless Concentration of Hydrogen at Pressures and Temperatures of Interest $(n_i No/VL_o)$(1) (From Ref. 10)

	100 Atmospheres			300 Atmospheres		
	H	H_2	H+ (2)	H	H_2	H+
293°K	10^{-30}	9.323E-01				
1000°K	6.181E-09	2.732E+01	--	1.1E-08	8.195E+01	--
2500°K	2.733E-02	1.090E+01	1.782E-17	4.737E-02	3.273E+01	1.364E-17
5000°K	2.552E+00	2.911E+00	6.299E-07	5.040E+00	1.135E+01	5.251E-07
23,000°K(2)	4.045E-01	4.291E-05	4.140E-01	1.796E+00	8.282E-04	9.614E-01

(1) n_i = moles of species i in the system

N_o = Avagadro's number

V = System volume in meter^3 (i.e., $\frac{n_i N_o}{V}$ = $\frac{\text{atoms or molecules of species i}}{\text{meter}^3}$)

L_o = 2.68699×10^{25} particles/meter^3 (Loschmidt number)

(2) Electron concentration is nominally the same as the H+ concentration

(3) Note, the 23,000°K values are shown merely for completeness. The calculations in this report were limited to a relatively low temperature demonstration test, and 5000°K temperatures for hydrogen were the highest employed.

by direct use of the classical scattering laws. The P_1 transfer matrices for transfers from the PHROG groups above the INCITE cutoff level of 2.38 eV were not developed, but complete P_1 transfer matrices for all of the INCITE groups (levels 13 to 19) were employed. The transport calculation was performed in S_4 detail using spherical geometry models and complete rational P_0 and P_1 scattering matrices, except as noted above.

3.2 Criticality Calculations

For the calculations, a general spherical model which consisted of a fueled core with radius 2/3 that of the cavity radius (Figure 3.1) was employed. The reactor was divided into 11 regions with 3 regions in the fueled volume of the cavity, 2 regions in the hydrogen coolant annulus, a one-region cavity wall, a one-region coolant inlet annulus, a two-region heat shield, and a two-region D_2O reflector. The mesh point spacing varied from region to region, but was the same for all the transport calculational cases. Table 3.3 summarizes the model dimensions used for the base case and Table 3.4 summarizes the case variations which consisted of dimensional changes and temperature and material atom density changes in regions in the cavity. Two additional preliminary transport cases which are not shown in the tables were calculated. These cases dimensionally were the same as case 1 but with fewer regions and an increased number of mesh points. The model was modified to assist the transport code to converge more efficiently and to reduce computer time without loss of accuracy. One of these early cases is of interest because atom densities used for the hot gases in the core and coolant regions were for 8000°K and 2500°K, respectively, but the hydrogen density in the 50% volume fraction cavity wall and in the inlet

Table 3.3

Model for Calculation of Base Reactor - Case No. 1

Region	Region Width (cm)	Outer Radius (cm)	Number Mesh Points	Region Materials
1	20.0		10	Vapor fuel* with 3% volume fraction H_2 Both at 200 atmospheres and 2500°K
2	8.0		5	Same as Region 1
3	5.333	33.3	10	Same as Region 1
4	8.667		5	H_2 at 200 atmospheres and 2500°K
5	8.0	50.0	5	H_2 at 200 atmospheres and 1000°K
6	2.0	52.0	3	BeO Cavity Wall 50% V.F. and H_2 at 200 atmospheres and 293°K - 50% V.F.
7	2.0	54.0	3	H_2 inlet annulus at 200 atmospheres and 293°K
8	4.0		11	BeO - 50% V.F. heat shield D_2O - 50% V.F., both at 293°K
9	12.0	70.0	8	Same as region 8
10	50.0		40	D_2O reflector at 293°K
11	40.0	160.0	20	Same as Region 10

* Fuel was the nominal metallic Oralloy composition of 93.2% U-235, 5.4% U-238, 0.4% U-234 and 1.0% U-236.

TABLE 3.4

Calculational Case Descriptions and Calculated Eigenvalues

(S_4 transport code -- 19-energy groups, full upscattering in seven "thermal" groups)

Case	Description
1	50-cm radius cavity with a fuel ball 33.33-cm radius. Fuel is 93.2% U-235 enriched with 1% U-236, 0.4% U-234, 5.42% U-238. All 3 fuel regions at 2500°K and 200 atmosphere pressure with a 3% by volume H_2 content at the same pressure and temperature. Hydrogen coolant inner region H_2 at 2500°K and 200 atmospheres. Outer coolant region at 1000°K and 200 atmospheres. Cavity wall region 50% by volume BeO and 50% by volume H_2 at 293°K and 200 atmospheres. H_2 inlet annulus region at 293°K and 200 atmospheres. Heat sheild regions, 50% by volume BeO and 50% by volume D_2O at 293°K. D_2O reflector regions at 293°K. K = 0.970
2	Same as Case 1 except core region temperatures raised to 5000°K and fuel and H_2 densities in the core reduced to 1/2 the values for Case 1. K = 0.909
3	Same as Case 2 except that fuel and H_2 volume fractions in the core regions are changed to 70% and 30%, respectively. K = 0.860
4	Same as Case 3 except the region widths in the hydrogen coolant regions 4 and 5 changed to 5 cm and 11.667 cm, respectively. K = 0.869
5	Same as Case 4 except cavity radius changed to 70 cm and region width for regions 1, 2, 3, 4, and 5 ratioed up from a 50-cm cavity to 70-cm cavity. 200 atmospheres. K = 0.923
6	Same as Case 5 except pressure raised to 400 atmospheres and fuel and hydrogen densities changed accordingly. K = 0.774
7	Same as Case 5, except 100 atmospheres. K = 1.0031
8	Same as Case 5 except fuel ball to cavity radius ratio changed to 0.8. K = 1.142

annulus were such as to correspond to lower temperature conditions (500°K and 373°K) with the system at 200 atm pressure. At the time these calculations were made, only the 5,000°K hydrogen cross section data had been generated. Thus, high temperature cross sections were then used with low temperature and these data were used in all regions containing hydrogen densities. This case dramatically illustrates the up-scatter effect of hot hydrogen, for it gives an eigenvalue of 0.78. The follow-on case used all room temperature hydrogen cross section data with all atom densities held constant, which resulted in a 31%Δk change in eigenvalue from 0.78 for the hot case to 1.09 for the cold case. It is obvious that the extreme penalty of 5,000°K hydrogen makes it impossible to achieve criticality at these temperatures in a 50 cm radius cavity at a radius ratio of fuel to cavity of 0.67. Cases 5, 6, and 7, Table 3.4, indicate that, contrary to the intuitive feeling that increasing pressure will increase K_{eff}, the total cavity pressure coefficient appears to be negative, at least in the range studied. Thus, increasing the cavity pressure will not compensate for raising the hydrogen temperature. Increasing the radius ratio to 0.85-0.90, as predicted in case 8, Table 3.4, could compensate for some of this reactivity deficiency. However, ratios of this magnitude are hydrodynamically difficult to achieve.

Diffusion theory was tried for preliminary scoping of cavity size. It was from these calculations that a preliminary cavity radius of 50 cm was deduced. The diffusion code used employed a fixed 19-energy group structure; however, only one thermal group was available in the code, with no thermal upscatter. Resonance self-shielding factors were included in the calculation for the fuel region. The model dimensions and atom densities were identical to the hot transport case mentioned above. The calculated eigenvalue using this code had agreed well with the room temperature critical experiments. However, with but a single

thermal group adjusted for total cross sections equal to the hot hydrogen, this code was woefully inadequate to calculate the hot hydrogen cases. The code could not account for the significant alterations that occured in the thermal neutron spectrum between the "cold" D_2O reflector-moderator and the hot hydrogen coolant. For instance, the hot case, calculated with the single thermal group, gave a multiplication factor of 1.006 compared to 0.78 for the multi-thermal group transport case. Essentially, this entire error was the result of inadequate treatment of hot hydrogen upscatter, not because of the differences between transport and diffusion theory. (Though the latter effect is not negligible, it is only the order of 5%Δk and hence small compared with the hot hydrogen upscatter effect.)

After reviewing the results given in Tables 3.3 and 3.4, NASA Lewis Research Center calculated the thermodynamic distribution of uranium and hydrogen atoms using their radiant heat transfer code. Using cavity dimensions of 4 ft diameter and low discharge and core-edge temperatures as assumed in the above nuclear calculations, NASA found that uranium temperatures in the core center were extremely high with resulting atom densities that were quite low. Figures 3.4 to 3.6 graphically represent the specified temperature, fuel, propellant, and propellant seeding distributions. This data essentially formed the base for developing atom densities for the second iteration of nuclear calculations. Tables 3.5 and 3.6 list the parameters initially used in the matching computer solutions. It will be noted that the specified radius ratio is still 0.67, however, the fuel densities are considerably less than used in the preceeding calculations. Of note, also, is the fact that no mixing of hydrogen with the fuel in the core has been assumed by NASA.

Table 3.7 shows the variations on the basic cases investigated, and the resultant criticality factors. The effect of U^{238} as the seeding material was

shown to be slightly negative, but not of sufficient magnitude to alter the results if omitted, so in subsequent runs no seeding material was included. Due to the expense involved in using the transport code SCAMP, a multi-thermal group diffusion theory code, MONA, which employed the same energy format and cross-section library as SCAMP, was used in most of the variations tested. Agreement between the two codes was within 1%Δk.

Using the atom densities and distributions specified by NASA, K_{eff} was found to be only 0.49 and 0.58 for the 500 and 200 atmosphere cases, respectively. These values are far from criticality. The bulk of the variations examined in this series of calculations used the 500 atmosphere case as a starting point, since the greater amount of fuel seemed to give the greater potential in ever becoming critical. This was assumed to be true despite the negative pressure coefficient from the base calclations.

The effect of fuel-propellant mixing in the core, which from the non-nuclear flow testing was known to occur, was investigated by mixing hydrogen with the uranium in various densities in the three fuel regions. It was assumed, reasonably, that the greatest amount of mixing would occur in the outermost fuel region, with lesser amounts of mixing in the inner two. There also exist temperature differences in these regions, and for the purposes of the mixing cases, hydrogen at 23,000°K was used in the inner two, and at 5,000°K in the outermost fuel region. In the mixing, it was assumed that at the specified temperatures in the fuel, the uranium would be doubly ionized. Thus, to keep the pressure constant, for every three atoms of hydrogen mixed into a core region, one atom of uranium, a nucleus and its two electrons, were removed. While the choice of doubly ionized was somewhat arbitrary, it was thought to be

conservative, based on extrapolations to published values for uranium plasmas. The cross sections for 23,000°K hydrogen were calculated for hydrogen atoms, since at that temperature, the molecules are nearly all dissociated. The results of this series of calculations are shown in graphical form in Figure 3.7.

The deleterious effect of hot hydrogen was further checked by including a thin region of 23,000°K hydrogen in the propellant region next to the fuel, replacing the 5,000°K hydrogen atom for atom. This dropped K_{eff} by 10%Δk. Since this design effort was to correspond as closely as reasonable to the expected mixing conditions, the effect of mixing 5,000°K hydrogen in the core instead of 23,000°K in the inner two regions was not checked in this series.

Although radius ratios larger than 0.67 become more difficult to maintain fluid-dynamically (at least in small cavities), the calculations have shown that in order to have an economically attractive sized demonstration test (i.e., about 4 ft diameter) of the gas core reactor concept, it apparently will be necessary to attempt to operate at higher radius ratios. Opacity studies of seeded hydrogen as coolant have shown that minimal thickness of about 3 inches can be tolerated for low temperature (approximately 8,300°K) plasma operation. allowing larger radius ratios, up to approximately 0.9, to be feasible. The non-nuclear flow testing[19] has also shown that it may be possible to obtain such a larger value of radius ratio through proper selection of cavity parameters.

Further study is also needed in the area of fuel density distributions. The NASA specifications show a marked fuel density peaking at the outer edge of the fueled regions, due ostensibly to condensation of the gaseous fuel through interaction with the cooler propellant. The calculations have shown

sensitivity to the total fuel mass in the cavity, necessitating an exact knowledge of the actual fuel density distribution configurations.

To ascertain the effect on criticality of increasing the cavity radius at constant radius ratio, some variational calculations were performed on the basic cavity configuration, increasing each of the regions within the cavity proportionately, holding the reflector thickness constant. The graph in Figure 3.8 shows the results of this series. The radius ratio was chosen to be 0.90 in each of these cases. The flattening of the curve indicates that improvement on containment and radius ratio must be the dominant goal of further non-nuclear flowing gas cavity testing, if the ultimate goals of reasonably sized test cavity reactors is to be obtained.

In an effort to qualitatively ascertain the sign of the change associated with varying the temperature of the hydrogen in the reflector, the last two cases listed were calculated. In case #36, the core was unchanged from the preceding 10' diameter case, and the 293°K hydrogen in the reflector was replaced with 5000°K hydrogen. This increased k_{eff} from 0.890 to 1.230. In case #37, the 1000°K hydrogen in the cavity, as well as the 293°K hydrogen in the reflector was replaced with 5000°K hydrogen, the atom densities in each region being arbitrarily held constant. This changed k_{eff} from 0.890 to 1.172. These last two cases indicate that additional effort must be made in properly designing and specifying the reactor parameters chosen for the test configuration, in order to have meaningful correspondence between calculations and reality.

Additional graphical results are displayed in Figures 3.9 to 3.11. The dependent variable displayed in some of these figures, the effective radius R_{eff}, is defined to be a region fuel density weighted average radius,

$R_{eff} = \frac{\Sigma\ \rho_i\ (4\pi\ r_i^2\ \Delta r_i)\ x\ r_i}{\Sigma\ \rho_i (4\pi\ r_i^2\ \Delta r_i)}$. Low values of k_{eff} shown indicate strongly the need for further investigation of cavity reactor parameters prior to final design of a test reactor configuration.

Table 3.5

S_4 Transport Code-19 Energy Groups, Full Upscattering in 7 Thermal Groups

500 atmospheres - NASA Distribution Specs - Base Case No. 1

Region	NMP	Material	Conc.		Thickness (width)(cm)	Radius (cm)
1	20	H (23,000°K)	0		35.00	35.00
		U-234	1.846×10^{-7}	0.018 gm/cc		
		U-235	4.301×10^{-5}			
		U-236	4.615×10^{-7}			
		U-238	2.492×10^{-6}			
2	10	H (23,000°K)	0		9.00	44.00
		U-234	2.256×10^{-7}	0.022 gm/cc		
		U-235	5.257×10^{-5}			
		U-236	5.640×10^{-7}			
		U-238	3.046×10^{-6}			
3	5	H (5,000°K)	0		2.86	46.86
		U-234	4.717×10^{-7}	0.046 gm/cc		
		U-235	1.099×10^{-4}			
		U-236	1.179×10^{-6}			
		U-238	6.368×10^{-6}			
4	10	H (5,000°K)	2.410×10^{-3}	0.004 gm/cc	14.14	61.00
		U-238	2.564×10^{-6}	0.001 gm/cc		
5	10	H_2 (1000°K)	4.519×10^{-3}	0.015 gm/cc	9.00	70.00
		U-238	1.282×10^{-5}	0.005 gm/cc		
6	5	H_2 (293°K)	4.06×10^{-3}		2.00	72.00
		BeO	3.624×10^{-2}			
7	5	H_2 (293°K)	2.444×10^{-3}		2.00	74.00
8	30	D_2O	3.624×10^{-2}		16.00	90.00
		BeO				
9	40	D_2O	3.31×10^{-2} + 0.0022% H		50.00	140.00
10	20	D_2O	3.31×10^{-2} + 0.0022%H		40.00	180.00

The atom densities given above, except for the U-238 seeding in regions 4 and 5 will be taken as a concentration of 1.0 for the balance of the models, unless explicitly stated. The atom density of 23,000°K hydrogen corresponding to a concentration of 1.0 will be taken to be that of the hydrogen in region 4, 2.410×10^{-3} atoms/barn cm. The fuel is Oralloy - 93.2% U-235, 5.4% U-238, 1% U-236, and 0.4% U-234. All subsequent cases unless explicitly stated, used identical reflectors, that is, regions 6-10 were the same in most cases. These regions correspond to those used in previous calculations also.

Table 3.6

200 Atmospheres - NASA Specifications - Base Case No. 2

Region	NMP	Material	Conc.	Thickness (width)(cm)	Radius(cm)
1	20	H (23,000°K)	0	35.00	35.00
		U-234	8.922×10^{-8}		
		U-235	2.079×10^{-5}		
		U-236	2.230×10^{-7}		
		U-238	1.204×10^{-6}		
2	10	H (23,000°K)	0	9.00	44.00
		U-234	1.230×10^{-7}		
		U-235	2.867×10^{-5}		
		U-236	3.076×10^{-7}		
		U-238	1.661×10^{-6}		
3	5	H (5000°K)	0	2.86	46.86
		U-234	2.871×10^{-7}		
		U-235	6.690×10^{-5}		
		U-236	7.178×10^{-7}		
		U-238	3.876×10^{-6}		
4	10	H (5000°K)	7.531×10^{-4}	14.14	61.00
		U-238	6.409×10^{-7}		
5	10	H_2 (1000°K)	1.807×10^{-3}	9.00	70.00
		U-238	5.127×10^{-6}		

6-10 same as Case No. 1

Table 3.7

SUMMARY OF NASA SPECIFICATION CALCULATIONS

Item		k_{eff}
	SCAMP by Transport Code Cases (Refer to explanations at bottom of Table 3.6)	
1.	500 atmos. base case,seeded Hydrogen, No mixing of hydrogen in the fuel	0.488
2.	200 atmos. base case,seeded Hydrogen, No mixing of hydrogen in the fuel	0.581
3.	200 atmos. base case,seeded Hydrogen, Some mixing of hydrogen in the fuel	0.414
4.	500 atmos. base case,no seed,Hot H band,No mixing of hydrogen in the fuel	0.386
	MONA Diffusion Code Case	
5.	500 atmos. base case, no seed, no mixing of hydrogen in the fuel, slightly simplified reflector	0.452
6.	Same, except Region 3 radius 47.77 cm	0.485
7.	Same, except Region 3 radius 55.50 cm	0.763
8.	Same, except Region 3 radius 62 cm	0.982
9.	Same, except some mixing of hydrogen in Region 3, U conc. = 0.9	0.979
10.	Same, except mixing in Region 2 U conc.=0.9 and Region 3 - U conc. = 0.8	0.974
11.	Same, except mixing in Region 1 - U conc.=0.9, Region 2 - U conc. = 0.8, Region 3 = U conc. = 0.7	0.955
12.	Same, except mixing in Region 1 - U conc.=0.8, Region 2 - U conc.= 0.8, Region 3 - U conc. = 0.5	0.930
13.	Same, except mixing in Region 1 - U conc.=0.5, Region 2 - U conc.= 0.4, Region 3 - U conc. = 0.1	0.819
14.	Same as base case # 1, except fuel concentration = 0.5 and no seed in propellent region	0.285
15.	Same, except fuel conc. = 7.78	0.679
16.	Same, except fuel conc. = 9.00	0.700
17.	Same, except fuel conc. = 13.04	0.773
18.	Same, except fuel conc. = 50.94	1.729
19.	Same except fuel conc. = 20.64	0.930
20.	Same, except fuel conc. = 23.98	1.011
21.	Same, except fuel conc. = 23.51	0.999
22.	Same as #18, except fuel conc. = 2.0	0.521
23.	Same, except fuel conc. = 1.0	0.410
24.	Same as # 1, except Region 1 has Mat. 2 fuel Region 2 radius 56.00 cm, Region 3 radius 59.84 cm	0.776
25.	Same, except Region 2 radius 61, Region 3 radius 64.92 cm	0.961
26.	Same, except Region U conc. 1.6, Region 2 U conc. 1.4, Region 3 U conc. 1.0 Some mixing of hydrogen in fuel	0.439
27.	Same, except Region 1 U conc. 0.8, Region 2 - U con. 0.7, Region 3 U conc. 0.5 Some mixing of hydrogen in fuel	0.326
28.	Same as #18, except Region 1 radius 45.00 cm, Region 2 radius 60.00 cm, Region 3 radius 63.00 cm	0.862
29.	Same, except cavity radii radius = 78.18 cm	0.870
30.	Same, except cavity radius = 89.50 cm	0.884
31.	Same, except cavity radius = 91.44 cm	0.888
32.	Same, except cavity radius = 106.68 cm	0.894
33.	Same, except cavity radius = 121.92 cm	0.895
34.	Same, except cavity radius = 137.16 cm	0.890
35.	Same, except cavity radius = 152.4 cm	0.890
36.	Same, except hot Hydrogen in all reflector regions	1.230
37.	Same, except atom densities Same as #1	1.171

(Note: in all mixing cases, hydrogen densities were chosen to make up for fuel removed.)

26

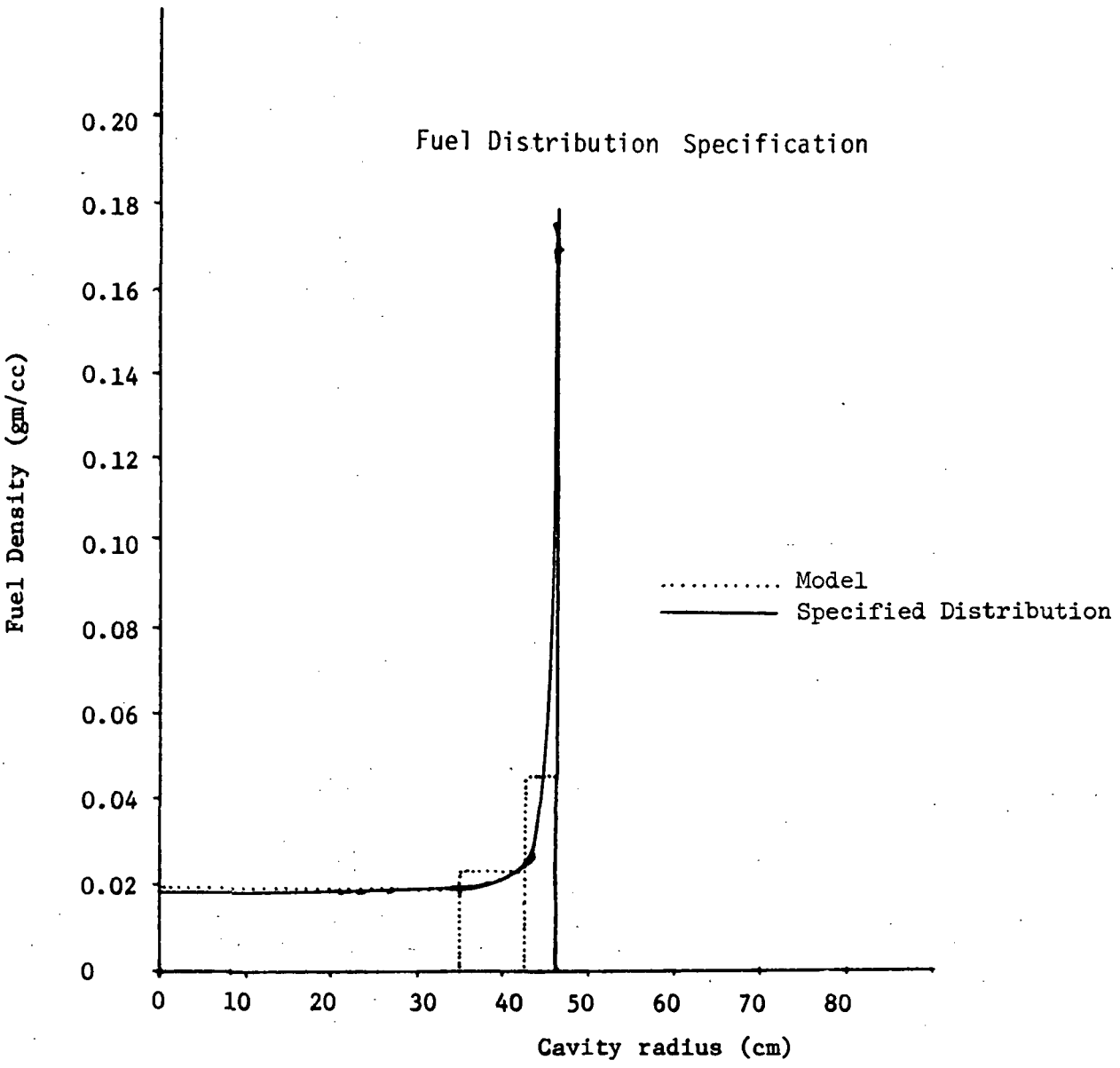

Fig. 3.4 NASA 70 cm cavity reactor fuel density distribution 500 atm pressure case (Model indicates the distribution assumed for the computer solutions.)

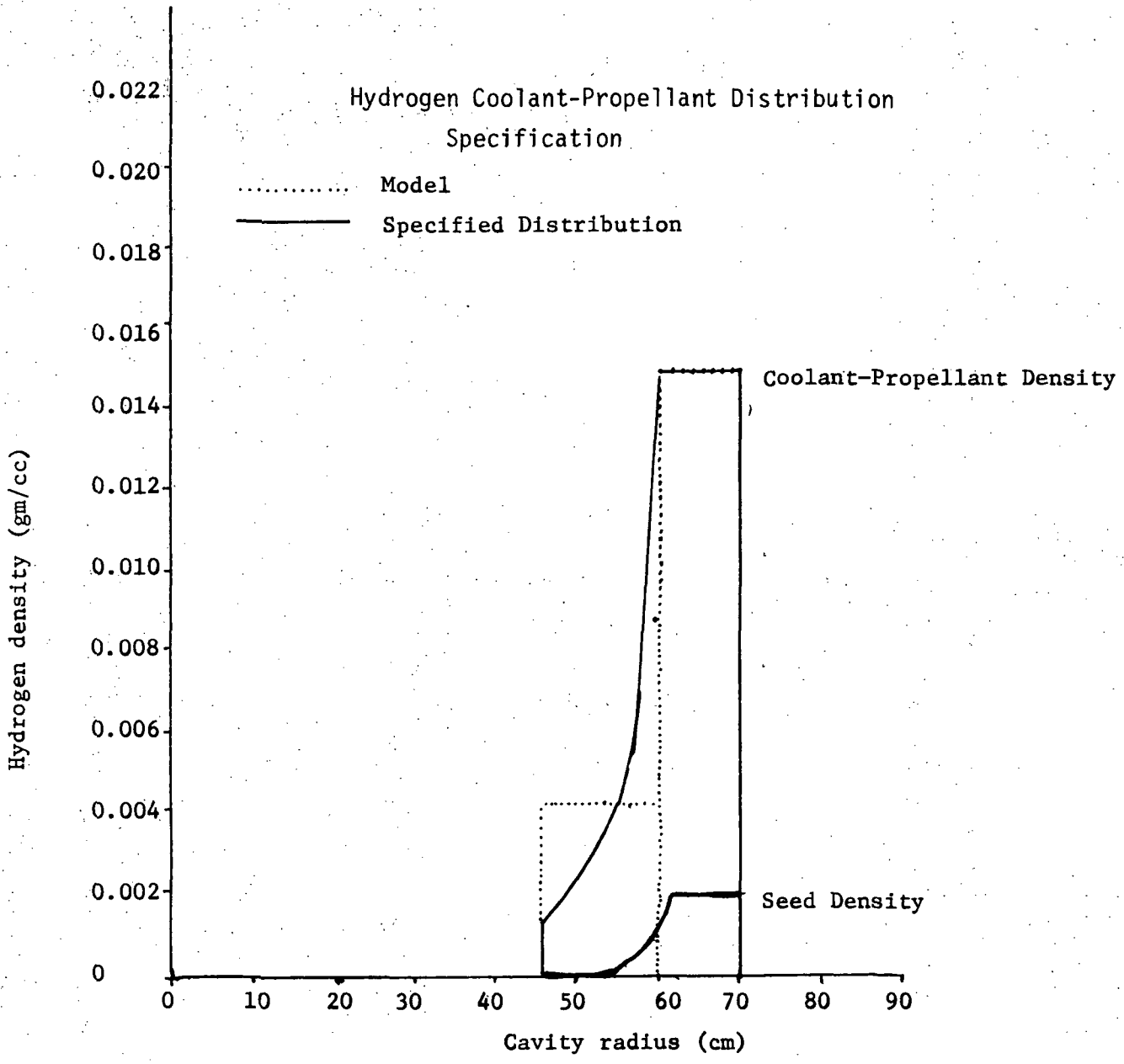

Fig. 3.5 NASA 70 cm cavity reactor hydrogen coolant-propellant density distribution - 500 atm pressure case (Model indicates the distribution assumed for the computer solutions.)

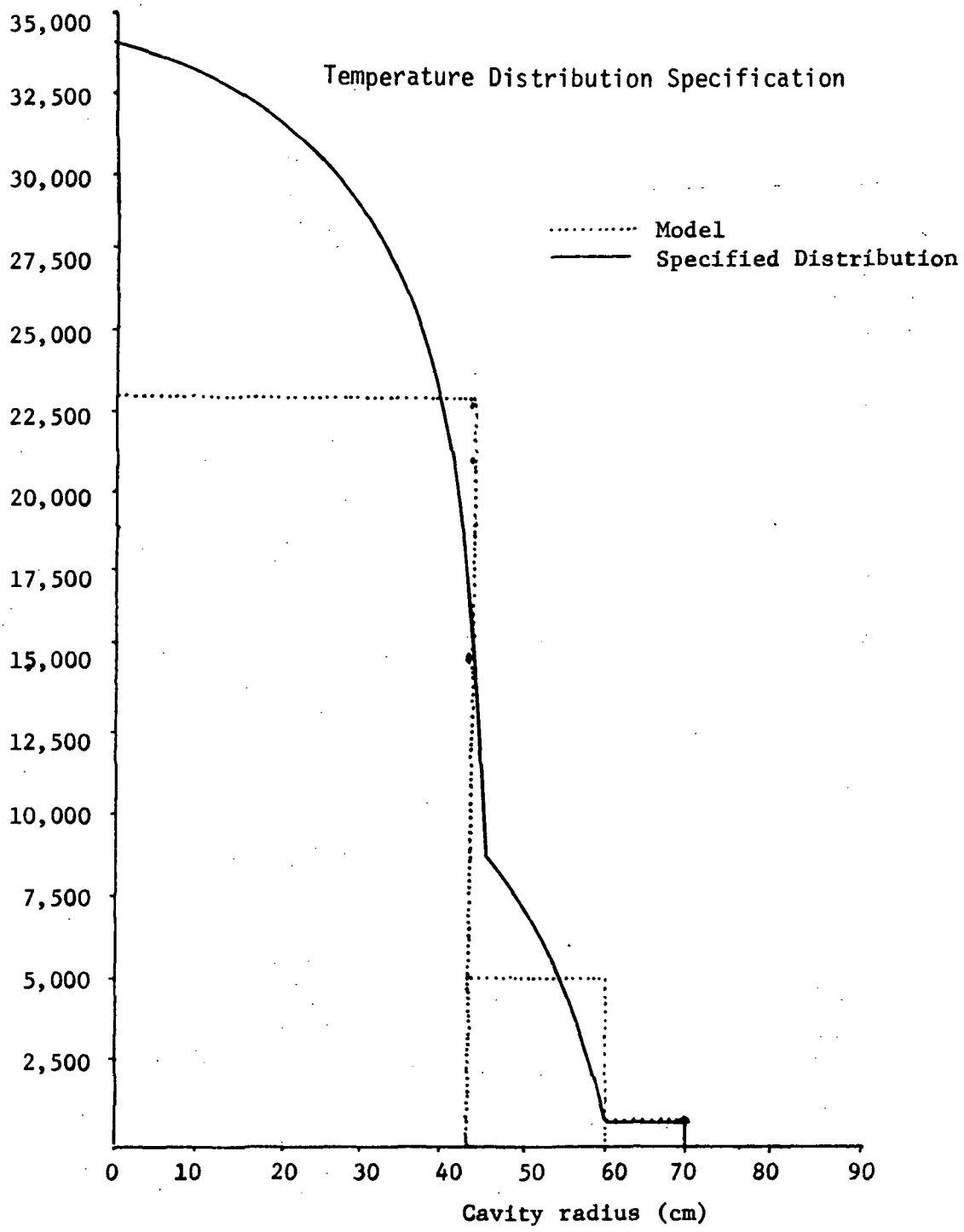

Fig. 3.6 NASA temperature distribution for 70 cm cavity reactor 500 atm case

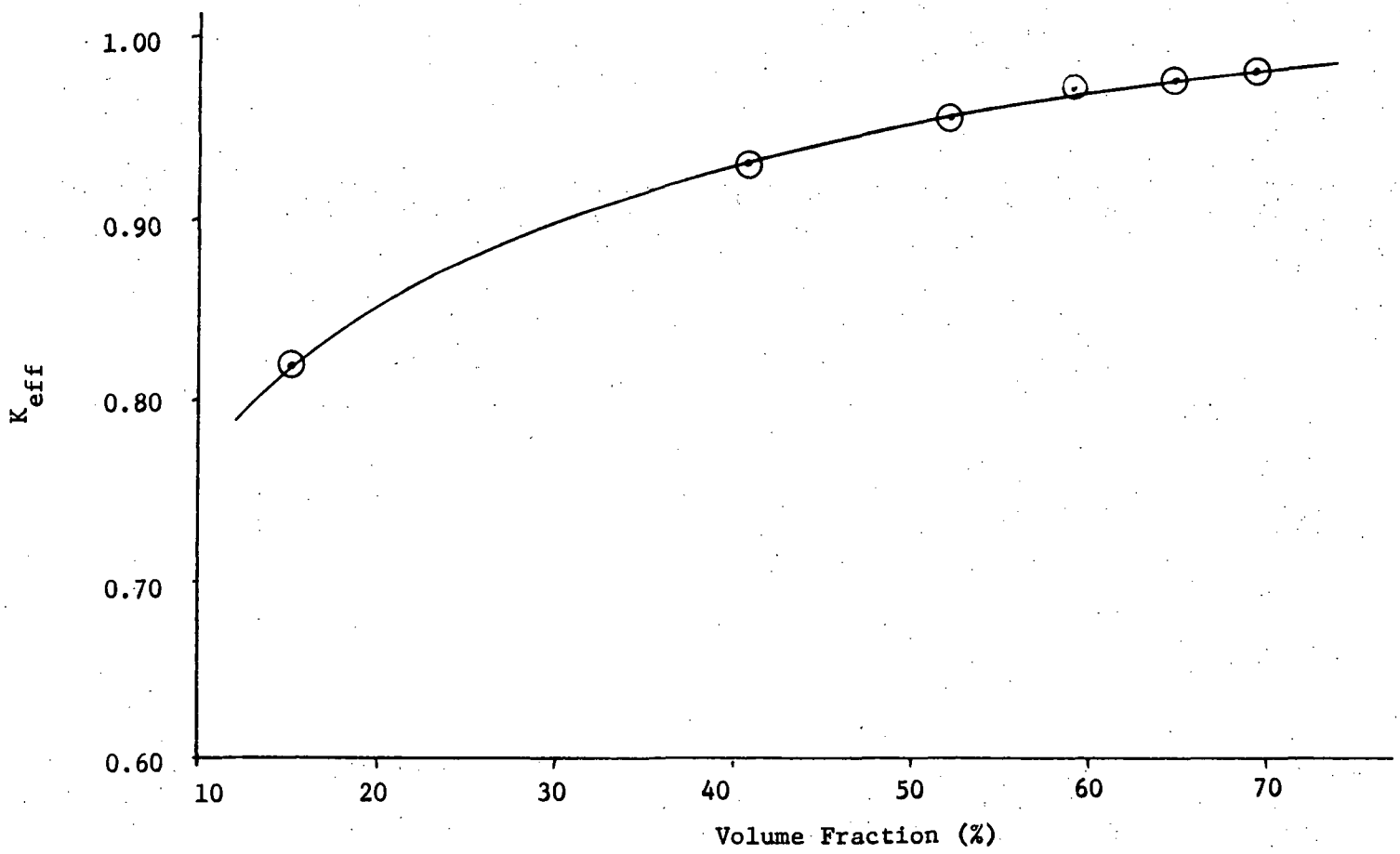

Fig. 3.7 MONA - NASA Specification Results K_{eff} vs volume fraction at constant radius ratio

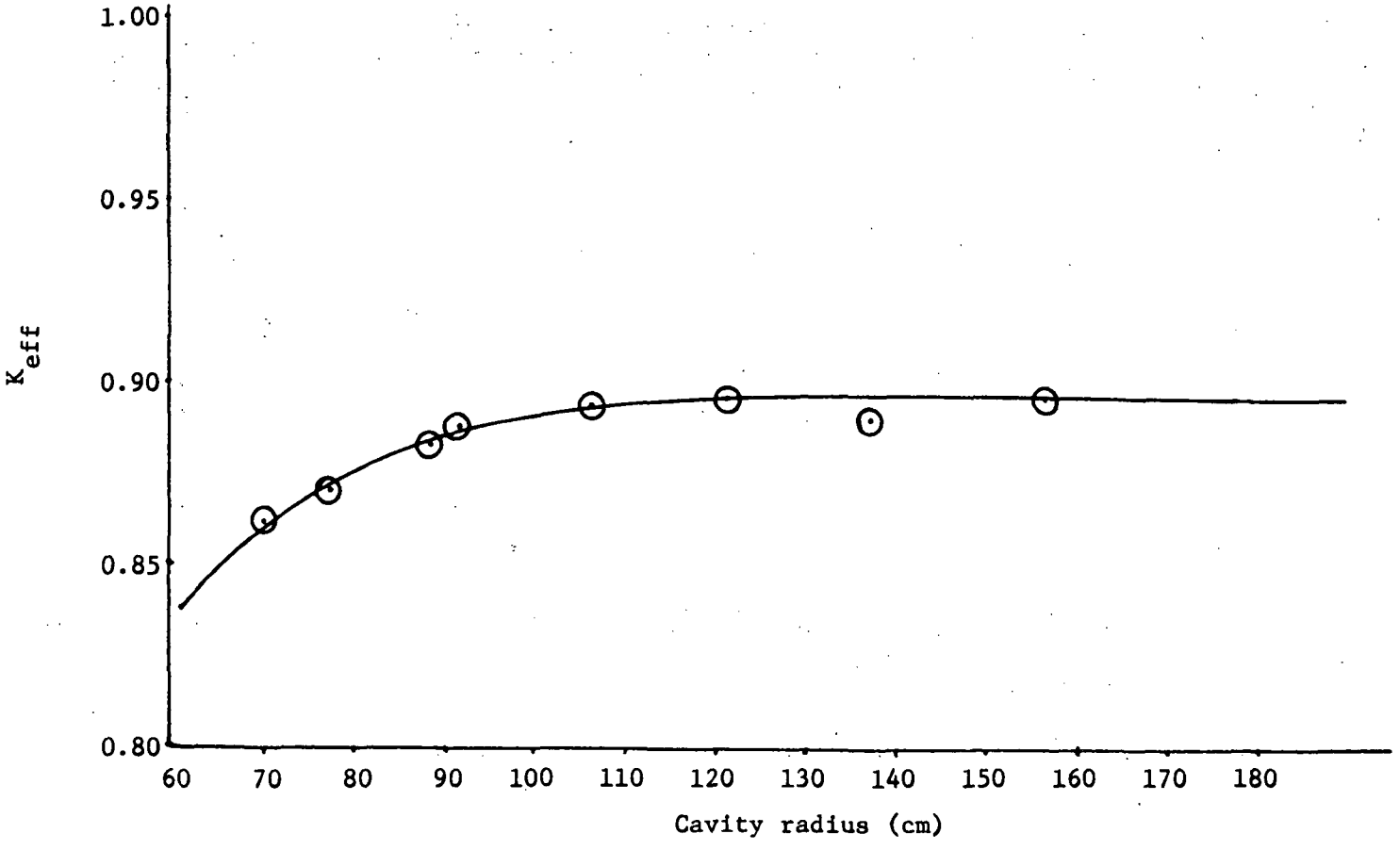

Fig. 3.8 MONA - NASA specification results K_{eff} vs cavity radius at constant radius ratio (Reflector thickness constant)

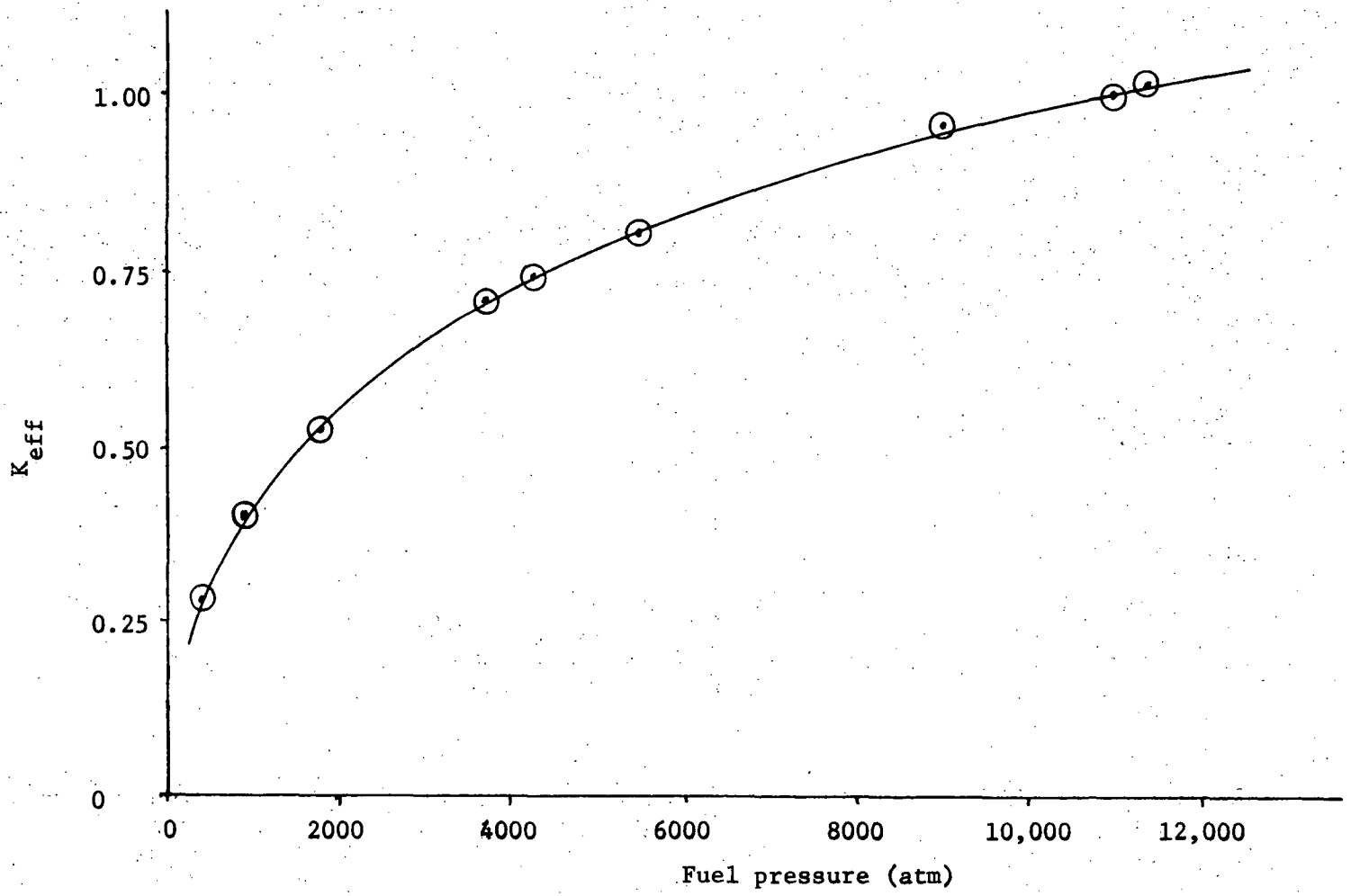

Fig. 3.9 MONA - NASA specification results K_{eff} vs fuel pressure at constant configuration and constant hydrogen parameters.

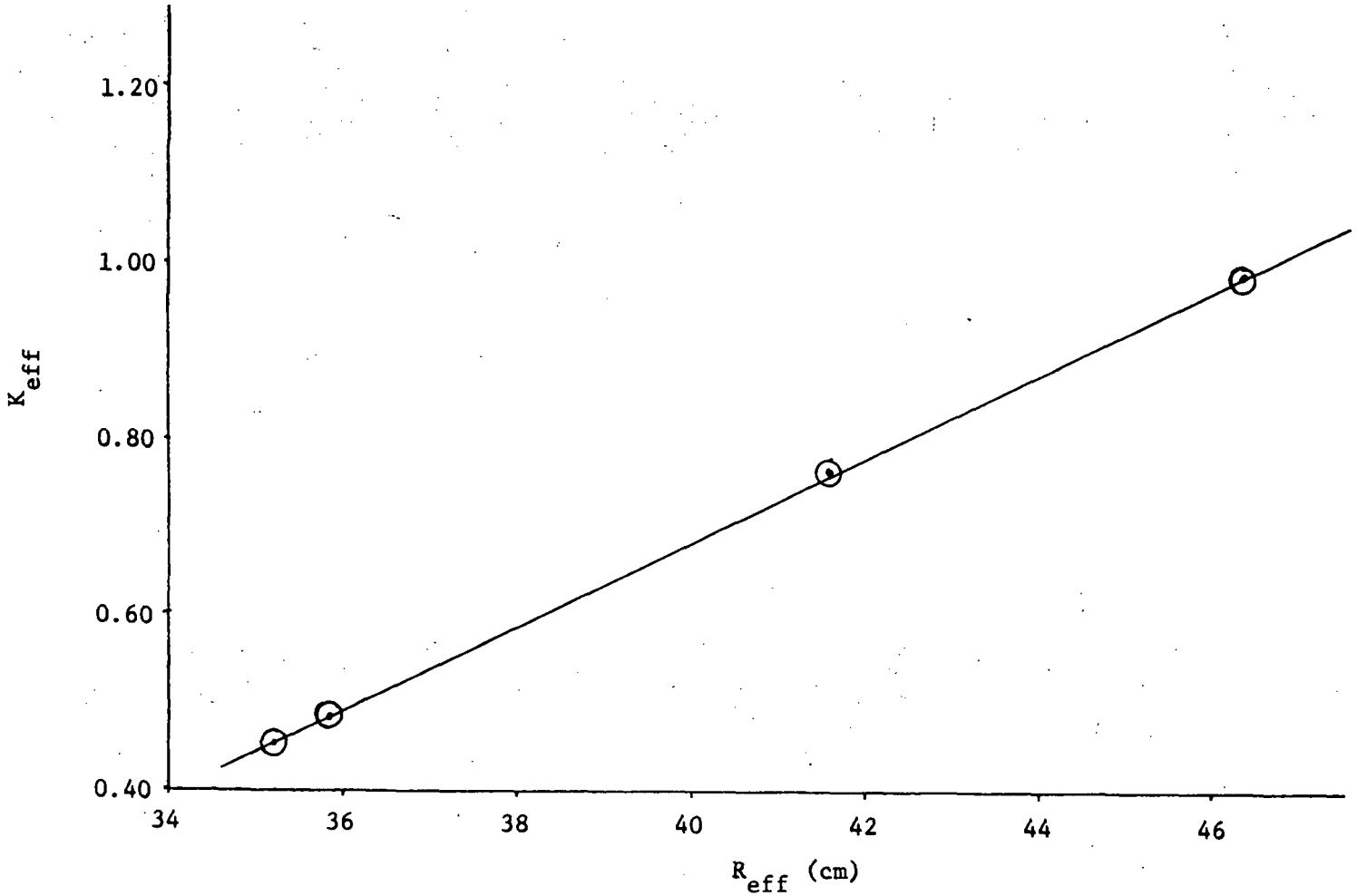

Fig. 3.10 MONA - NASA specification results K_{eff} vs R_{eff} at changing fuel mass

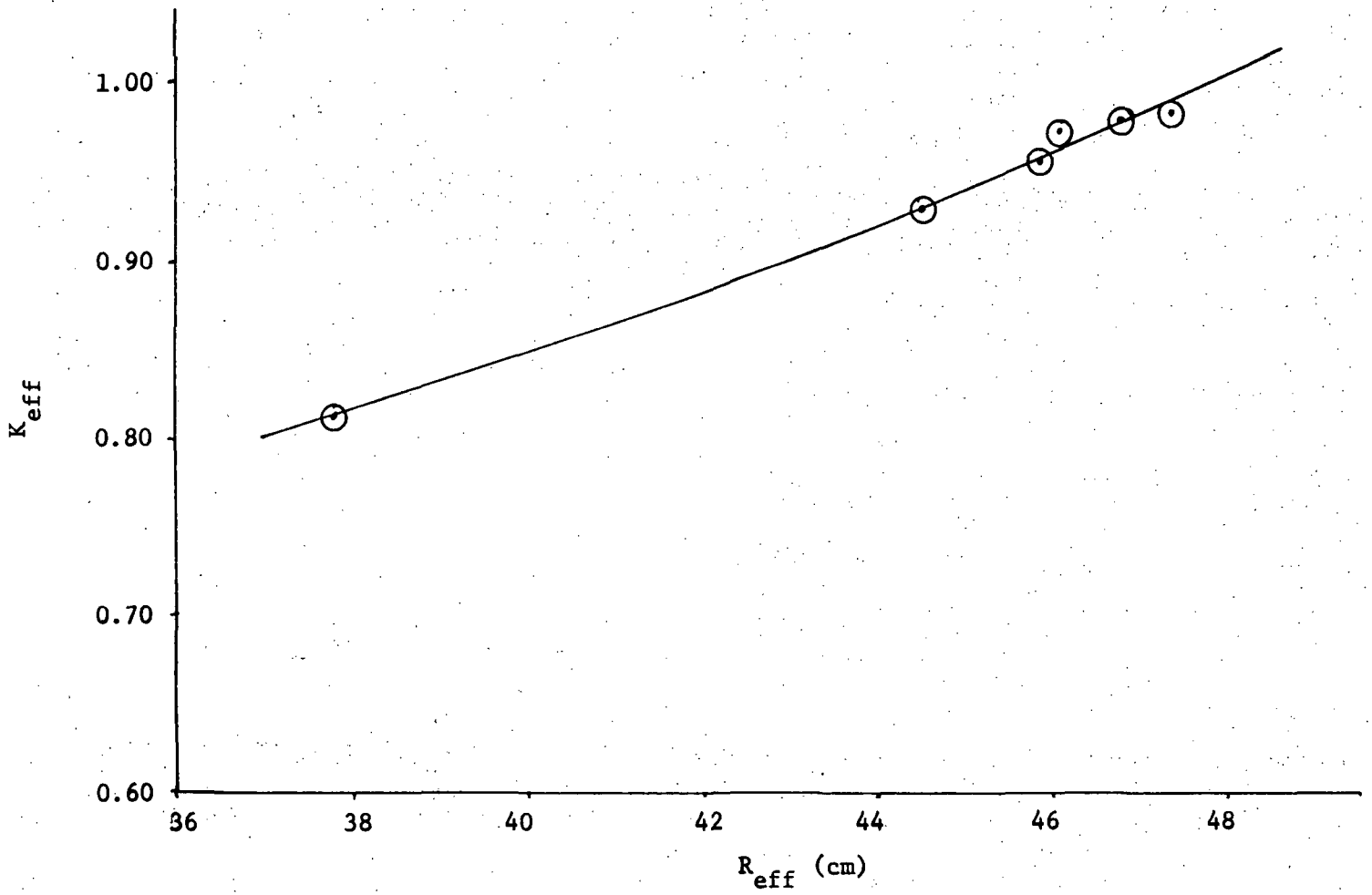

Fig. 3.11 MONA - NASA specification results K_{eff} vs R_{eff} at constant radius ratio

3.3 Temperature Coefficient

Total temperature coefficient arises from two main sources in the system, the temperature of neutrons returning from the reflector-moderator, and the up-scattering from hot hydrogen in the system. The reflector-moderator coefficient was not calculated but previous measurements in a cavity reactor critical experiment[7] give an indication of the magnitude and sign for this effect. For a system with a somewhat larger effective cavity volume in cylindrical geometry, with the same reflector-moderator thickness as was used in this series of calculations (Table 3.4) the measured average temperature coefficient from 32°C to 70°C was -0.0115% ΔK per degree centigrade rise in moderator temperature. During the same experiment and similar spherical geometry critical experiments,[9] the cold hydrogen penalty for an effective annulus 30-cm thick, containing 1×10^{21} of cold H atoms per cc surrounding the fuel was measured as approximately -7 to -12% ΔK. The penalty is less in systems with greater structural poison and hence greater fuel loading. This hydrogen atom density is in the range of the values used in the calculations in this report.

The combination of absorption and high scattering properties of hydrogen appears to impose this rather severe reactivity penalty. This penalty is drastically enhanced by elevating the hydrogen propellant temperature to that proposed for the test conditions. The enhancement is due to up-scatter in energy of thermalized neutrons returning from the reflector-moderator. The upscattering increases the energy and reduces the cross section for absorption interactions with the gaseous-fueled core. Figure 3.3 graphically illustrates how the total scattering cross section for the H_2 molecule increases with temperature. The scattering effect is strongest on those neutron energies most effective in the fission process

(ie, the lowest energy having the highest fission cross section), and consequently their loss to the fueled region of the cavity results in a strong negative hydrogen temperature coefficient.

Table 3.8 gives the calculated P_o macroscopic scatter cross section transfer matrix, by group, for the 8 lowest energy neutron groups used in the calculations. (The group energy structure is shown in Table 3.1.) This table compares the in-group and group-to-group transfer of neutrons in a hydrogen molecule environment at 2500°K and at 293°K temperatures at 200 atmospheres pressure. This quite clearly illustrates the importance of hydrogen upscatter on the system reactivity. Observe from the table that the hot H_2 cross section is greatest for up-scatter to group 14 (0.2 to 0.414 eV) from all of the lower energy groups, which is to be expected since 3/2 KT for a 2200°K effective neutron temperature is 0.28 eV. At this energy, the fission cross section on ^{235}U is only 73% of the room temperature cross section.

Finally, Figure 3.12 is a plot of the flux distribution in the 6 lowest energy neutron groups as a function of the cavity radius for Case 4 of Table 3.4. This calculation was based on a cavity pressure of 200 atmospheres with the fuel region containing 30% by volume H_2 and 70% by volume fuel at 5000°K. The surrounding hydrogen coolant blanket was divided into two zones, the inner most, 5-cm thick zone at 2500°K and the 11.667-cm thick outer zone at 1000°K. The curves show a steep loss of neutrons to the fuel below 0.08 eV. This loss shows up in an enhancement of neutrons in the higher energy groups, with group 14 showing the most marked increase due to up-scatter contributions from the lower energy groups.

Table 3.9 lists by energy group the average mean free scattering path lengths for both hot and room temperature hydrogen at 200 atmospheres of pressure. It is apparent that thermal neutrons returning from the reflector-moderator

Table 3.8

P_o Group to Group Scattering Matrix for Hot and Cold H_2

(The Upper Number is for 2500°K H_2, The Lower Number is for 293°K H_2)
(Both conditions at 200 atmospheres pressure)

Row	12	13	14	15	16	17	18	19
12	1.00E-02	1.10E-02	1.19E-03	4.47E-04	2.23E-04	3.05E-04	1.13E-04	2.79E-05
	4.27E-02	4.69E-02	5.10E-03	1.90E-3	9.52E-04	1.30E-03	4.83E-04	1.19E-04
13	1.64E-04	1.78E-02	4.97E-03	1.56E-03	6.67E-04	6.96E-04	1.45E-04	1.39E-05
	0.00E-00	5.89E-02	2.65E-02	9.45E-03	4.55E-03	5.51E-03	1.34E-03	1.35E-04
14	9.21E-07	7.91E-03	1.36E-02	6.53E-03	2.74E-03	2.84E-03	5.88E-04	5.61E-05
	0.00E-00	1.73E-04	2.96E-02	3.93E-02	1.89E-02	2.36E-02	6.08E-03	6.37E-04
15	8.63E-07	7.24E-03	1.30E-02	9.35E-03	4.71E-03	4.87E-03	1.01E-03	9.60E-05
	0.00E-00	5.53E-07	2.91E-03	3.54E-02	3.28E-02	4.10E-02	1.07E-02	1.13E-03
16	9.01E-07	7.52E-03	1.34E-02	1.01E-02	6.53E-03	7.37E-03	1.52E-03	1.45E-04
	0.00E-00	9.91E-08	5.20E-04	1.25E-02	3.67E-02	6.21E-02	1.62E-02	1.72E-03
17	1.12E-06	9.35E-03	1.65E-02	1.24E-02	8.37E-03	1.34E-02	3.39E-03	3.23E-04
	0.00E-00	2.78E-08	1.47E-04	3.54E-03	1.42E-02	8.69E-02	3.65E-02	3.88E-03
18	1.79E-06	1.49E-02	2.61E-02	1.96E-02	1.32E-02	2.30E-02	9.06E-03	1.03E-03
	0.00E-00	1.58E-08	8.60E-05	2.08E-03	8.36E-03	8.31E-02	9.00E-02	1.24E-02
19	3.83E-06	3.19E-02	5.58E-02	4.20E-02	2.82E-02	4.91E-02	2.20E-02	4.40E-03
	0.00E-00	2.35E-08	1.30E-04	3.17E-03	1.28E-02	1.27E-01	1.79E-01	5.24E-02

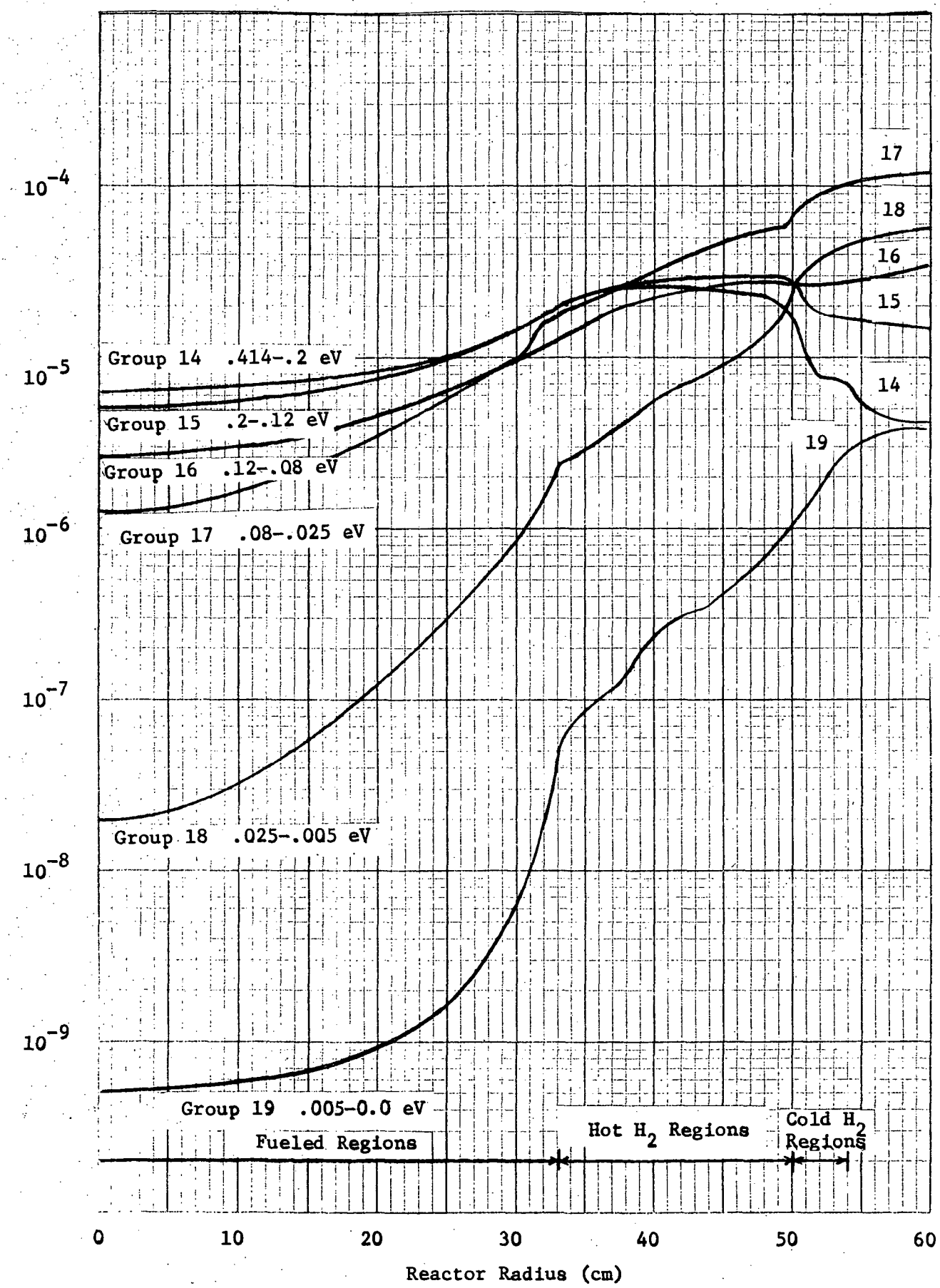

Fig. 3.12 Plot of some thermal neutron group flux data vs reactor radius through core and hydrogen containing regions for Case 4.

Table 3.9

Nominal Total Scattering Cross Sections and Scattering Mean Free Path for Thermal Neutrons in H_2

		2500°K H_2 gas - .000573 $\frac{H_2}{b\ cm}$		
Group	Energy (eV)	σ $\frac{barns}{H_2\ molecule}$	$\sum_s$ cm^{-1}	λ_s cm
19	0 - .005	550	.315	3.17
18	.005 - .025	210	.120	8.31
17	.025 - .08	110	.063	15.9
16	.08 - .12	78	.0447	22.4
15	.12 - .20	70	.0401	24.9
14	.20 - .414	60	.0344	29.1
13	.414 - 2.38	50	.0287	34.8

		293° H_2 gas - .00489 $\frac{H_2}{b\ cm}$		
Group	Energy (eV)	σ $\frac{barns}{H_2\ molecule}$	$\sum_s$ cm^{-1}	λ_s cm
19	0 - .005	180	.880	1.136
18	.005 - .025	90	.440	2.27
17	.025 - .08	60	.293	3.41
16	.08 - .12	52	.254	3.93
15	.12 - .20	50	.245	4.90
14	.20 - .414	45	.220	4.54
13	.414 - 2.38	42	.205	4.87

to the fuel may encounter an H_2 layer several mean free paths in thickness. Except for absorption and backscattering, this is not important for cold hydrogen. However, as discussed above, up-scattering becomes increasingly important as the hydrogen temperature is raised. The resulting temperature coefficient of reactivity effect can effectively limit the exhaust temperature and power level since it is a negative feedback effect. On the advantageous side, this temperature coefficient is also a very effective system stabilizer from a safety standpoint limiting both the system temperature and pressure.

3.4 Summary of Nuclear Results

It is obvious that the penalty of hot hydrogen to achieving criticality is most severe. The negative reactivity-temperature coefficient is in the range of -7%Δk per 1,000°K of discharge propellant temperature. Furthermore, the larger the cavity the higher will be the system multiplication factor for given conditions of temperature, pressure, and radius ratio. Thus, for larger cavities, higher operating temperature and discharge temperature will be possible. The calculations were not done in sufficient number to create a family of curves of exhaust temperature vs cavity size for various fuel to cavity radius ratios. However, the work performed indicates that the temperature vs cavity radius coefficient is approximately as given above.

From the series of calculations performed for this study, the 70-cm radius (4-1/2 ft diameter) cavity size appears to provide satisfactory conditions. Further study could lead to systems of this size showing promise of attaining criticality through hydrogen perheating or reflector design modifications. However, the brief nature of this study precluded further investigation that would allow exactly specifying the needed cavity size. Several iterations between the nuclear and radiant heat transfer codes are required.

The thermalhydraulic design in the following section was based on a 4 ft diameter cavity, as were the associated rough cost estimates. It appears that this size of reactor may be adequate for a useful demonstration test. There is little doubt, however, that the 4 ft cavity diameter size is indeed marginal, and a somewhat larger size would be desirable. However, this study was brief and cursory, and the nuclear calculation results should be used only as a guide.

Perhaps the most startling result from the study is that the pressure coefficient of reactivity is negative, at least for the conditions assumed in the study. This further illustrates that the hydrogen penalty is indeed severe, so much so that above 100 atmospheres the addition of more

fuel via an increase in pressure was more than counteracted by the negative effect of the corresponding increase in hydrogen. Certainly, the negative pressure coefficient will not be true at all pressures and temperatures, and a more complete study appears warranted.

Finally, the effect of a change in radius ratio of fuel to cavity is much stronger than hitherto assumed. Measurements of the effect in a "cold critical experiment[7] without hydrogen showed approximately a 6% ΔK increase in reactivity as the fuel ball radius increased from 0.67 to 0.80 of the cavity radius. With hot hydrogen as a coolant surrounding the fuel ball, the identical change in radius ratio was calculated to be 22% ΔK (cases 5 and 8 of Table 3.4). The reasons for the difference are that with hot hydrogen, growth of the fuel ball not only has a positive geometric effect on reactivity but also displaces some of the extremely deleterious hydrogen coolant from the cavity. This net effect would appear to be a strongly positive contribution to the reactivity temperature coefficient. However, the larger fuel radius is probably unstable fluid-dynamically,[15] and should quickly reduce back to its original size. Furthermore, the pressure and hydrogen temperature coefficients of reactivity are both negative. Thus, it would appear that overall the temperature effect on reactivity is negative.

4.0 THE CLOSED CYCLE TEST SYSTEM

A closed cycle test system is needed from environmental and economic considerations, since the gases passing through the test cavity will contain fission fragments. Release of fission fragments to the environment cannot be tolerated under present political conditions which demand very careful controls to avoid violating the environment. The necessary containment and clean-up equipment for a closed coolant loop, however, should cost less than the cost of the equipment for filtering out the uranium for re-use. Since the propellant gas will be re-used with a resulting cost savings, the complete containment system will not be such a major cost factor that it would dictate that the testing would be economically unfeasible.

4.1 Materials Selection

The selection of structural materials for the reactor are indeed critical. Nuclearly, the system must use as many low cross section materials as possible, since thermal neutrons will typically traverse the reactor several times before a fission reaction is likely. Selection of moderator-reflector material is also critical. Though beryllium and heavy water are both effective moderators for this system, the slight advantage of heavy water dictates its use as the main moderator. Beryllium or BeO would make fine heat shields within the D_2O moderator system.

The cavity wall should have low absorption properties as well as high temperature capabilities. The use of low melting temperature materials such as Al or Mg for the demonstration test is inappropriate until the cooling and temperature protection capability for the wall is demonstrated. Among materials that would be feasible are beryllium oxide, alumina, aluminum silicate, and clad zircaloy. Construction techniques for

the wall need to be developed. Tubular construction as well as photo-etching techniques would be considered. Note that construction of a spherical "porous wall" with tangentially directed flow will involve techniques that are not conventional. The geometric shapes will be difficult to define, specify and fabricate. Figure 3.1 shows a typical design that utilizes low cross section, high temperature materials, and Table 4.1 summarizes the types and characteristics.

4.2 Choice of Coolant Gas

Table 4.2 contains the coolant gases considered and their thermodynamic and nuclear properties of concern. Either hydrogen or a gas which approximates hydrogen's thermodynamic and nuclear properties is needed since hydrogen is necessary for the actual rocket engine to provide the required specific impulse. The disadvantage of using hydrogen is that its chemical reactivity creates an explosion hazard. However, hydrogen systems have been built and operated successfully.

If another gas were to be considered, its thermodynamic flow characteristics would have to be similar to those of hydrogen in order to provide a useful demonstration of the gas core concept at high temperatures. These thermalhydraulic requirements imply low molecular weight for the specific impulse and the gas-to-uranium-weight ratio. This consideration makes helium the only gas reasonable for approximating hydrogen thermalhydraulically for the gas core demonstration test.

The disadvantage of helium is that its nuclear properties differ considerably from hydrogen. As has been shown in Section 3, hydrogen's scattering properties have a strong effect on the nuclear system operation. Hydrogen's up-scattering capability is about 4 times that of helium while

Table 4.1

Materials Selection

Component	Materials for Consideration	Comments
1. Gas Core	a. Uranium Metal, vaporized for high temperature	A compound increases the pressure required for same U density
	b. Uranium metal dust or UF_6 gas for startup	Either dust or UF_6 will have a substantial gravitational effect and will require a specially designed feed and distribution system that is retractable when high temperatures are reached.
2. Cavity Wall (spherical and porous, with flow direction tangential) Little pressure drop. 2 to 4 inches thick	BeO, Al_2O_3	Ceramics with high temperature capability but difficult to fabricate and very brittle
	Aluminum Silicate	2000°F capability easily fabricated into honeycomb shapes
	Zirconium clad with Nb or alumina (Al_2O_3)	High temperature capability, high strength, easily fabricated
3. Hydrogen flow plenum boundary	Be or BeO about 4 inches thick	Heat shield capability also. Some structural integrity.
4. Reflector	D_2O, pressurized to cavity pressure with operating temperatures in the range of 500°F	Best all-around reflector material
5. Reflector Structure	Zircalloy or Mg	Strength and low cross section
6. Outside pressure shell, approximately 10 ft diameter for 3000 to 6000 psia	Stainless clad carbon steel	Probably modified cylindrical-spherical shape using conventional pressure vessel technology. A major-cost item.

Table 4.2

Characteristics of Coolant Gases

Gas	Molecular wt.	Thermal Absorption Cross Section (barns)	Thermal Scatter Cross Section (barns)	Specific Heat at 1000 F Btu/lbm °F	Thermal Conduct. at 1000 F Btu/hr ft°F	Absolute Viscosity at 1000 F lbm/sec ft	Activation
H	1.008	0.332	38*	3.4	0.23	12×10^{-6}	None
He	4.003	$\leq$ 0.05	0.8	1.2	0.16	25×10^{-6}	None
O	16.00	< 0.0002	4.2	0.24	0.03	25×10^{-6}	None
N	14.01	1.85	10	0.27	0.034	24×10^{-6}	None
Ne	20.18	0.032	2.4	$\sim$0.2	--		Little
Ar	39.95	0.63	1.5	0.125	--		Ar 40 to Ar 41 β (1.83 hr) to K 41

* At room temperature. At higher temperatures, the atomic (unbound) cross section of 20 barns prevails.

its cross section for scattering is approximately 25 times higher. Therefore, a test facility designed with helium will differ significantly from a hydrogen rocket design.

It is apparent that a hydrogen gas test facility will make the greatest possible advancement in gas core rocket technology. The use of helium would indeed compromise the significance of the results. Therefore, hydrogen was chosen for this preliminary design study, and it is felt that its choice will extend well beyond this preliminary work.

4.3 The Gas Cycle

The closed hydrogen cycle shown in Figure 4.1 includes: (1) a constant high pressure liquid or gaseous hydrogen supply to the cavity, (2) nozzle coolant supply, (3) system for cooling the hot exhaust gas, (4) system to remove the uranium and the seed material from the gas stream, (5) filters for removing fission products, (6) exhaust gas storage tank, (7) compressor and liquifier to repressurize and liquify the coolant (hydrogen) gas, and (8) water coolant for the heat exchanger. For a 4-ft diameter cavity, a hydrogen mass flow rate of 3 lb_m/sec is needed to maintain a volumetric flow rate of 1600 ft^3/min at 200 atm pressure. The total hydrogen mass flowing through the cavity for a three minute run is about 530 lb_m These conditions are those which model the full scale 10-ft diameter cavity rocket requirements, within a nominal 4-ft diameter cavity demonstration test.

The constant high pressure supply can be obtained by blowdown from high pressure storage tanks or from a compressor. To supply the 530 lb_m of hydrogen for blowdown a pressure vessel of 500 ft^3 is required at a pressure 200 atmospheres greater than the test cavity pressure. To

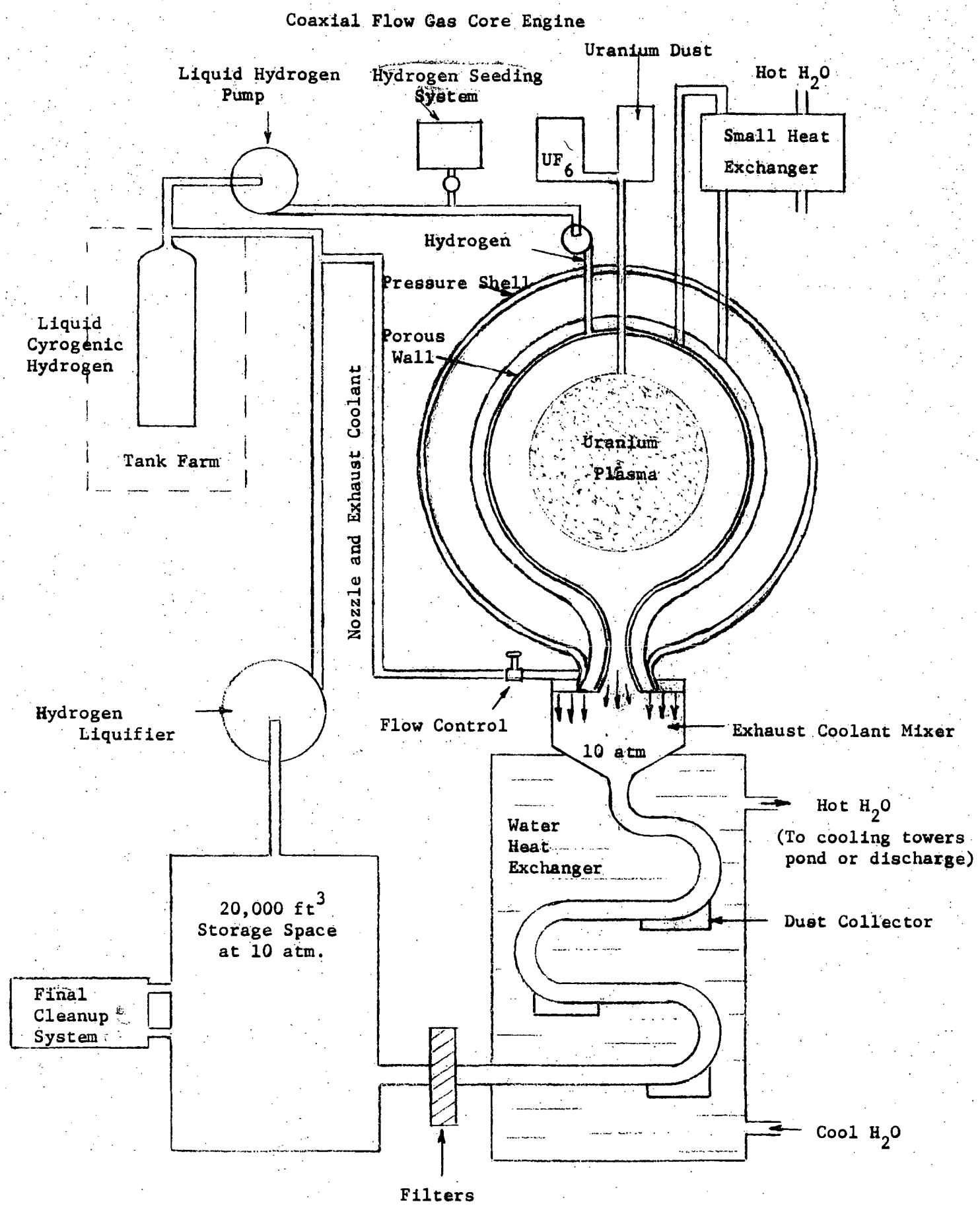

Fig. 4.1 Closed Cycle Test System

pressurize 3 lb_m/sec hydrogen flow rate from 1000 psia to 6000 psia (400 atm) requires a compressor of about 5000 hp. A feedback pressure control system is needed to regulate constant pressure to the cavity and nozzle.

The large requirements for the hydrogen gas feed system have led to the consideration of liquifying the gas before re-cycle. Pumping requirements for the liquid are in the range of 500 hp. Liquid hydrogen will also be used in the actual rocket application, and hence its use in the demonstration test will make the test more pertinent to the actual application. Use of the liquid storage is also likely to result in lower overall capital costs for the complete hydrogen system. Before the hydrogen enters the cavity, it will be seeded by an appropriate material (such as tungsten - Ref. [4]) to provide the coolant with the needed attenuation coefficient for radiant energy.

The exhaust hydrogen from the nozzle is cooled by two means. First, cool hydrogen* is injected into the exhaust stream to cool the exhaust hydrogen enough so that high temperature requirements are tolerable; and secondly, a water cooled heat exchanger will remove sufficient energy to bring the gas to nominally ambient temperature. A mass flow rate of cool hydrogen equal to the nozzle exhaust rate injected at the nozzle exit will cool the exhaust from 5000°R to 2750°R. The exhaust gas from the nozzle is ejected at mach one from a throat area of 0.7 $in.^2$. After mixing at 20 atm pressure, an average velocity of about 3200 fps is obtained, which requires an exhaust chamber of about 4-in. diameter.

*This exhaust stream coolant will consist of half of the total hydrogen mass flow requirements. However, the coolant diluent need only feed into a 20 atm system, and the pumping requirements for this flow will be negligible compared to the required for the cavity coolant.

The hydrogen next passes through a heat exchanger consisting of a serpentine pipe of 4-in. nominal diameter designed to trap the uranium and seed. The heat exchanger piping will be adequately borated with partitions to prevent criticality. Finally, high efficiency particulate filters would be used to remove anything not trapped in the heat exchanger. The cooled and cleaned gas is then stored in a low pressure tank of about 23,000 ft^3 total volume at 10 atm. Another feedback pressure control system is needed to regulate a constant pressure in the hydrogen exhaust system. This control is primarily for protection of the discharge collection and clean-up system. The critical pressure ratio for choked-flow nozzle discharge makes discharge pressure control in the range of 1 to 20 atm of little importance to the performance of the reactor.

4.4 The Gas-Uranium Separation System

The gas-uranium separation system must remove the uranium from the hydrogen exhaust stream and be constructed so that the uranium can be removed remotely from the system at the end of each run. The idea presented here is to make use of the large difference in the masses of hydrogen and uranium molecules and the resultant centripetal forces.

The method is to use a tube-in-shell type heat exchanger in which the hydrogen and uranium flow is through the tubes and the water coolant flows through the baffled shell. The tubes are made into one continuous tube by joining them external to the shell. Each external joint will be a 180-degree turn in which centripetal forces are applied to the uranium. This forces the uranium dust to the outside walls of the joints where traps will be placed to catch the uranium. After each run the joints can be

removed to extract the uranium without completely disassembling the heat exchanger. The radiation levels will necessitate that this operation be performed remotely.

The mixing of uranium and hydrogen as hot gas, and the subsequent cooling of these gases for separation of the two materials raises the question of the formation of uranium hydride. Ref. [17] discusses the formation of metallic uranium hydride (UH_3) with the release of ~30.3 Kcal/mole, and the dissolution of hydrogen gas in the molten uranium. Neither problem appears to be serious enough to be of major concern in the operation of the gas core demonstration. Hydriding of the metal can be anticipated to the extent of 1 atom of hydrogen per 2000 atoms of uranium in the cooled metal at atmospheric pressure. Higher concentrations in the ratio of the square root of the pressure can be anticipated for the discharge nozzle down stream conditions, where design pressures as high as 20 atm are specified. Above 435°C, the uranium hydride metal decomposes and the problem then turns to one of dissolution in the molten uranium. The information in Ref. [17] leads to the conclusion that a relatively rapid cooling of the uranium-hydrogen gas mixture will result in only a fractional atom percent of hydrogen atom concentration in the uranium.

4.5 Cavity Wall Thermal Hydraulics

The pressure drop in the hydrogen inlet annulus between the cavity wall and the heat shield is approximately 10 psia or less due to friction. The mach number was estimated at 0.01 to 0.1, therefore, the pressure can be assumed to be the stagnation pressure. The maximum hydrogen flow velocity calculated is 130 ft/sec at the inlet. The spherical geometry, the decreasing mass flow rate and the increasing temperature and friction

will change the angular velocity of the hydrogen around this annulus. Consequently, the orificing of the cavity wall will need to be carefully pre-established and specified in cold-flow component tests.

Heat transfer coefficients for the sides of the cavity wall were calculated using the Dittus-Boelter correlation for turbulent flow of nonmetallic fluids through ducts and tubes. With an annulus velocity of 40 ft/sec at 600°F, the heat transfer coefficient calculated for the annulus is 930 Btu/hr ft^2F. For a 1 ft/sec at 5000°F flow along the inside cavity wall and 1 ft/sec at 620°R transpiration cooling flow through the wall, the heat transfer coefficient for the inside wall has been estimated[18] to be 0.7 Btu/hr ft^2F.

The maximum cavity wall temperature calculated using the above heat transfer coefficients is about 1000°F at the inside surface of the cavity wall for a thermal radiation heat flux of 100 W/cm^2 (3.17 x 10^5 Btu/hr ft^2), a cavity gas temperature of 5000°R, and an outer flow-distribution annulus gas temperature of 600°R. The calculation neglected the gamma heating in the cavity wall and the convective transfer from the 5000°R hydrogen in the cavity. The gamma heating was estimated to be less than 10%[18] of the 100 W/cm^2 and the convective heat transfer from the 5000°R cavity wall is less than 1% using the above heat transfer coefficient. Based on these assumptions, the outside and inside wall temperatures are 480°F and 1000°F, respectively. The peak wall temperature will be on the inside surface unless this temperature exeeds the effective fluid (gas) temperature. The radiant heat flux is the most predominant factor contributing to high wall temperatures. The 1000°F temperature is tolerable for high temperature ceramic type materials or refractory metals, but would be completely unacceptable for aluminum or magnesium.

5.0 OPERATING CHARACTERISTICS

The startup method would utilize a cold hydrogen gas flow into the cavity. A specially designed injector would be inserted into the cavity to introduce and disperse the fuel in the cavity, into a shape compatible for criticality. Once nuclear operation commenced, the power level would gradually be increased until the desired temperatures were obtained for vaporization of uranium metal. At such time, the uranium feed system would be switched to a pellet or dust high velocity injection system operating from outside the cavity. The startup injector would then be withdrawn from the cavity.

5.1 Power Levels and Temperatures

To achieve the desired 4000°R minimum discharge temperature at 1600 ft^3/min of hydrogen gas at 200 atm of pressure, a cavity power level of 35 to 40 MW is required. Higher temperatures and pressures will result in correspondingly higher total powers. The 1600 ft^3/min is the flow rate found to be necessary in cold flow component tests[15] with a similar sized cavity. Much lower flows result in conditions that do not adequately expand the inner gas to the volume needed for criticality.

Because of the strong temperature coefficients of reactivity, large swings in reactivity control will be needed. However, this control of the reactor can easily be established by reflector control mechanisms,[16] with worths in the range of 15 to 20% ΔK. The long prompt neutron lifetime ($\sim$2 milliseconds) makes the reactor relatively safe and controllable even under prompt critical conditions.

The reactor will need to be operated by indirect observation of the nuclear conditions. Exact flow and geometry conditions within the cavity will not be observable, and must be deduced indirectly. Consequently, the most sophisticated reactor kinetics control and analysis systems will need to be employed. On-time noise analysis of a variety of signals will be essential.

5.2 Radiation Levels

The mode of operation will be similar to that of NERVA and ANP tests. The control room will be physically separated from the test area for the reactor. Following a test, the reactor and certain auxiliary components will be transported to a hot shop. Essentially no reactor shielding will be necessary

The short periods of operation -- several minutes a test and perhaps only 2 or 3 hours total in a year -- will result in low activation levels. If plate out of fission products can be kept to a minimum, the servicing problems should be relatively easy once the fission products extracted from the exhaust stream are removed. However, flux levels will be in the range of 10^{16} thermal n/cm^2 so that direct manual operation on reactor components will not be possible even if no residual contamination exists.

5.3 Test Changes, Servicing and Maintenance

The principal servicing operations will consist of operation of the uranium and hydrogen clean-up and recharging systems. This will comprise the main activity between the brief power tests. Recharging and preparation for a rerun (no alterations to the reactor) will probably require a minimum period of one working week.

5.4 Diagnostics

Since the purpose of these tests is to study all aspects of the gas core reactor concept, the means of diagnostics will probably be varied and extensive and due consideration of these needs will be given to diagnostics in the design. The diagnostics must cover, among other things, the neutronics and criticality of the reactor; the hydrodynamics of the core, propellant and coolant; the behavior of the vessel walls and structural materials; the thrust generated; the fuel injection; the radiation and energy transport. This will require an extensive array of probes. For instance, the size of the core and the flux distribution within the core might be determined by a fast neutron hodoscope.

6.0 COST AND SCHEDULE ESTIMATES

The following tabular estimate of costs is based on rough estimates of construction and operation of the 4-ft diameter cavity demonstration test at a test site where there are existing utilities, roads, and support facilities. The first column shows our cost estimates based on our experience with similar facilities (not an engineered cost estimate) and the second column shows our estimates of the cost difference between this full-reactor demonstration test and the Mini-Cavity test. It is this latter column that should be of more significance, since the cost difference estimates are likely to be more meaningful and accurate than the absolute cost estimates. A 4-year minimum schedule from the start of Title-I design until operation can begin should be assumed.

For the estimated annual operating cost of $5,000,000., an operating organization of about 80 personnel could be supported. This would allow the conducting of several (2 or 3) major test configuration changes within a one-year period. The costs quoted in this section are to be considered for planning purposes only.

Table 6.1

Primary Construction Costs of 4 ft. Cavity Demonstration Reactor

Component	4-ft Cavity Reactor Estimated Cost	Estimated Difference Between 4-ft Cavity and Mini-Cavity Cost	Comments
Reactor Vessel (external)	$2,000,000	+$1,700,000	Based on costs of similar-sized LWR pressure vessels
Cavity Wall	1,000,000	+ 300,000	Mostly fabrication costs
Primary Heat Exchanger(s)	4,000,000	- 1,000,000	Includes remotely removable uranium traps
Secondary Coolant System	500,000	0	Short-period operation capability makes this a minor design problem
Hydrogen Storage System For Discharge Gas	2,000,000	+ 1,000,000	20 atm; capacity = 23,000 ft^3
For liquid hydrogen	500,000	+ 200,000	
Hydrogen Liquifier	1,500,000	+ 500,000	
Hydrogen Pumps and flow control system	3,000,000	+ 600,000	
Partial Flow Cleanup System	1,500,000	+ 500,000	
Hot Waste System	2,000,000	0	
Uranium Reprocessing System	500,000	0	
Exhaust Nozzle and Discharge System	1,500,000	+ 200,000	
Absolute Filters	100,000	0	
Reactor Structure (general including Be & BeO)	2,000,000	+ 500,000	
Uranium Feed System	500,000	0	Both metal dust injection and startup (cold) systems
Seeding System for Hydrogen	300,000	0	Tungsten seed
Explosion-proofing protection	1,000,000	+ 300,000	
Control System	1,000,000	0	

Table 6.1 (Cont'd)

Component	4-ft Cavity Reactor Estimated Cost	Estimated Difference Between 4-ft Cavity and Mini-Cavity Cost	Comments
Data System	$ 200,000	0	
Handling and transport system to hot shop	(existing)	0	The NERVA and ANP concept of railrod transport between test site and hot shop is assumed.
Shielding	None	50,000	
Safety Analysis, Quality Assurance, and Safety Review	500,000	0	
Miscellaneoua	1,000.000	0	
Fuel Element fabrication	0	- 250,000	
Fuel and D_2O	(no cost)	0	
Total Cost	$25,000,000	$4,600,000	more than the Mini-Cavity ($20.4 million)

Table 6.2

Operating Costs

Item	Cost	Difference Between Mini-Cavity	
Installation and Checkout	$300,000	$ ∿ 0	
Fixed Operating Annual Cost	$5,000,000	$ ∿ 0	Would include operating and maintenance crews and support services

7.0 CONCLUSIONS AND RECOMMENDATIONS

A full-reactor demonstration test with a 4-ft diameter cavity has been the subject of preliminary feasibility design calculations. The 4-ft size appears to be too small to achieve the required test temperatures. However, a small increase in size beyond 4-ft plus alterations in fluid-hydraulic test patterns should result in an adequate configuration. The cost of such a test is estimated to be approximately 25% greater than that of a Mini-Cavity test.

The limiting factor of the full scale test is the temperature that can be achieved, since hot hydrogen has an extremely deleterious effect on reactivity. However, the 4-ft cavity can probably achieve close to 4000°R discharge conditions, enough to adequately demonstrate feasibility of the gas core concept. In addition, this discharge temperature would be sufficient to drive a MHD generator, if such a demonstration were desired. The test by its very nature is an experimental investigation of a fissioning plasma.

Among the following recommendations, item 1 appears most needed before a decision on a full-reactor or a Mini-Cavity test is made.

1. The extremely strong hot hydrogen reactivity effect needs to be more thoroughly studied for all gas core concepts, including the Mini-Cavity.
2. Flow control to adjust the radius fuel-to-cavity ratio will be a strong effect on reactivity, and needs to receive additional study in non-nuclear flow tests.
3. Use of ^{233}U will enhance the multiplication factor and allow operation at higher temperatures. More attention to a study on its future availability would seem appropriate.

4. There is a possibility of providing additional reactivity in the use of fuel elements in the reflector. This results in a hybrid "Mini-Cavity" reactor, and probably deserves further consideration.

5. The mixing of hydrogen and helium as a coolant was not considered in this report. This would reduce the hydrogen reactivity penalty without sacrificing essential thermalhydraulic characteristics. Such a consideration deserves further attention.

REFERENCES

1. G. Safanov, "The Criticality and Some Potentialities of Cavity Reactors", (abridged), RM-1835, The RAND Corporation (1955).

2. F. E. Rom, "Comments on the Feasibility of Developing Gas Core Nuclear Rockets", NASA TM-X 52644, Conference on Frontiers of Power Technology, (October 23-23, 1969).

3. M. F. Taylor, et al, "The Open-Cycle Gas-Core Nuclear Rocket Engine-- Some Engineering Considerations", 2nd Symposium on Uranium Plasmas: Research and Applications, Atlanta, Georgia (November 15-17, 1971) p. 179.

4. W. R. Jacobs and J. R. Williams, "Measurement of Thermal Radiation Scattering Characteristics of Submicron Refractory Particles", 2nd Symposium on Uranium Plasmas: Research and Applications, Atlanta, Georgia, (November 15-17, 1971), p. 137.

5. R. E. Hyland, "A Mini-Cavity Probe Reactor", 2nd Symposium on Uranium Plasmas: Research and Applications, Atlanta, Georgia, (November 15-17, 1971) p. 261.

6. C. E. Vogel, "A Progress Report - Induction Plasma Simulation of the GCNR", 2nd Symposium on Uranium Plasmas: Research and Applications, Atlanta, Georgia (November 15-17, 1971) p. 170

7. J. F. Kunze, G. D. Pincock and R. E. Hyland, Nucl. Appl. 6, 104 (1969).

8. W. B. Henderson and J. F. Kunze, "Analysis of Cavity Reactor Experiments", NASA CR-72484 (January 1969).

9. J. F. Kunze, J. H. Lofthouse and C. G. Cooper, "Benchmark Gas Core Critical Experiment", Nucl. Sci. Engr. 47, pp. 59-65 (1972).

10. R. W. Patch, "Thermodynamic Properties and Theoretical Rocket Performance of Hydrogen", NASA SP-3069 (1971).

11. R. L. Curtis, and R. A. Grimesey, "INCITE - A FORTRAN IV Program to Generate Thermal Neutron Spectra and Multigroup Constants Using Arbitrary Scattering Kernels", Idaho Nuclear Corp., IN-1062 (1967).

12. R. L. Curtis, et al, "PHROG - A FORTRAN IV Program to Generate Fast Neutron Spectra and Average Multigroup Constants", Idaho Nuclear Corp. (April 1971).

13. G. D. Janou, et al, "GATHER-II: An IBM-7080 FORTRAN-II Program for the Computation of Thermal-Neutron Spectra and Associated Multigroup Cross Sections", GA-4132 (1963).

14. G. D. Janou and J. D. Dudek, "GAM-I: A Consistent P-1 Multigroup Code for the Calculation of Fast Neutron Spectra and Multigroup Constants", GA-1850 (June 1961).

15. J. F. Kunze et al, "Flowing Gas, Non-Nuclear Experiment on the Gas Core Reactor", NASA CR-120824 (Feb. 1972).

16. J. H. Lofthouse and J. F. Kunze, "Spherical Gas Core Reactor Critical Experiment", NASA CR-72781 (Feb. 1971).

17. V. S. Yemel'Yanov and A. I. Yevstyukhin, "The Metallurgy of Nuclear Fuel", (Pergamon Press, translated from the Russian, 1969), pp 78-84 and pp 140-142.

18. J. P. Holman, "Heat Transfer", (McGraw-Hill, 1963) p. 353.

19. J. F. Kunze et al., "Phase II Topical Report, Flowing Gas, Non-Nuclear Experiments on the Gas-Core Reactor," NASA CR-121191, ANCR-1118, June 1973.